Author/s:
Gayan, S;Senanayake, R;Inaltekin, H;Evans, J

Title:
Reliability Characterization for SIMO Communication Systems with Low-Resolution Phase Quantization under Rayleigh Fading

Date:
2021-01-01

Citation:
Gayan, S., Senanayake, R., Inaltekin, H. & Evans, J. (2021). Reliability Characterization for SIMO Communication Systems with Low-Resolution Phase Quantization under Rayleigh Fading. IEEE Open Journal of the Communications Society, 2, pp.2660-2679. https://doi.org/10.1109/OJCOMS.2021.3133526.

Persistent Link:
https://hdl.handle.net/11343/307901

This article has been accepted for publication in a future issue of this journal, but has not been fully edited. Content may change prior to final publication. Citation information: DOI 10.1109/OJCOMS.2021.3133526, IEEE Open Journal of the Communications Society

Reliability Characterization for SIMO Communication Systems with Low-Resolution Phase Quantization under Rayleigh Fading

Samiru Gayan, Rajitha Senanayake, Hazer Inaltekin and Jamie Evans

This paper investigates the communication reliability for single-input-multiple-output wireless systems with low-resolution phase quantizers. First, the maximum-likelihood detector with n-bit phase quantization is derived when there are N antennas at the receiver. Then, three low-complexity antenna selection strategies for data detection are proposed and their symbol error probability performance is characterized. It is shown that having 3 or more bits is sufficient to attain the full diversity order N, achievable with infinite-bit quantizers, for quadrature phase shift keying modulation under Rayleigh fading. In particular, it is established that the proposed low-complexity max-distance and max-norm antenna selection strategies perform the same as the maximum-likelihood detector in terms of the asymptotic system reliability for $n \geq 3$. On the other hand, the diversity order decreases dramatically from N to $\frac{N}{2}$ when n is equal to 2, as illustrated by our numerical results and proven for the case of $N = 2$. An extensive numerical and simulation study is performed to illustrate the accuracy of the derived results and asymptotic system reliability performance as well as verifying our hypotheses in the high signal-to-noise ratio regime.

***Index Terms*—Low-resolution quantization, ML detectors, selection combining, symbol error probability, diversity order.**

I. Introduction

A. Background and Motivation

Low-resolution analog-to-digital converter (ADC) based transceiver architectures have gained increasing attention both from the wireless industry and academia in recent years [1]–[4]. Some notable benefits of low-resolution ADCs in wireless communication are reduction in transceiver power consumption, simplification in system design (especially with 1-bit ADCs) and reduction in transceiver form-factor [2], [5], [6]. The importance of these benefits is becoming even *more* pronounced with the emergence of massive multiple-input multiple-output (MIMO) and mm-wave technology, which require large numbers of RF chains and high sampling rates. The stated benefits do, however, come with the cost of increased distortion in received symbols due to the high level of quantization noise, which eventually decreases the system reliability and achievable data rates [1], [7]–[9].

As an important step to characterize communication reliability with low-resolution ADCs, three reliability regimes were established in [8]. They can be called quantization *plateau*, *slow-decay* and quantization *invariance* regimes. In the quantization plateau regime, the number of quantization bits, n, is so small (when compared to the input signal alphabet size) that the system reliability cannot be improved by increasing the input signal power or the system signal-to-noise ratio (SNR). In this regime, the system diversity order (DVO), defined as the ratio of the logarithm of the symbol error probability to the logarithm of SNR as SNR grows large, collapses to zero. In the slow-decay regime, n is equal to the logarithm of the input alphabet size and the symbol error probability decays to zero *slowly* with SNR at a DVO that is half of the one achieved by high-resolution quantization. In the quantization invariance regime, n is larger than the logarithm of the input alphabet size and the DVO does not change with n. In this regime, we achieve the same DVO that can be achieved by means of a high-resolution quantizer. These fundamental structural results were *only* obtained for single-input single-output (SISO) low-resolution ADC communication systems in [8], and their extension to the multi-antenna systems is a completely open problem in the literature.

In this paper, we focus on the communication reliability characterization for a single-input-multiple-output (SIMO) wireless communication system in which the receiver is equipped with low-resolution phase quantizers. By using DVO as our main performance metric, we determine communication reliability to first order. We propose three low-complexity antenna selection strategies for data detection and we obtain reliability regimes for the proposed strategies, analogous to those obtained in the case of SISO systems in [8]. We establish their asymptotic optimality properties as a function of the quantization bits in terms of DVO, and compare their performance with the one achieved by the derived maximum likelihood (ML) detector. Similar to the SISO case, our results in this paper show that it is enough to use 3 bits to achieve the full DVO in the case of quadrature phase shift keying (QPSK) modulation (i.e., one additional bit on top of the logarithm of the input alphabet size) when the receiver is equipped with N antennas.

Our main contributions can be further summarized in detail as follows:

- Motivated by the capacity achieving property of circularly symmetric input distributions for low-resolution ADCs [9], [10], we focus on the QPSK modulation in this paper and derive the optimum ML detection rule with n-bit phase quantization for a SIMO system with N receive antennas. This result is presented in Theorem 1 and it is a generalization of the ML detector presented in [11] for multi-bit quantization. We show that the ML detector achieves the full DVO N for $n \geq 3$ when

Samiru Gayan is with the Department of Electronic and Telecommunication Engineering, University of Moratuwa, Katubedda, Sri Lanka. (e-mail: samirug@uom.lk).

Rajitha Senanayake and Jamie Evans are with the Department of Electrical and Electronic Engineering, The University of Melbourne, Parkville, VIC 3100, Australia. (e-mail: rajitha.senanayake@unimelb.edu.au, jse@unimelb.edu.au.)

Hazer Inaltekin is with the School of Engineering, Macquarie University, North Ryde, NSW 2109, Australia. (e-mail: hazer.inaltekin@mq.edu.au)

This article has been accepted for publication in a future issue of this journal, but has not been fully edited. Content may change prior to final publication. Citation information: DOI 10.1109/OJCOMS.2021.3133526, IEEE Open Journal of the Communications Society

the channel is subjected to Rayleigh fading (i.e., see Theorem 5). By using numerical simulations, we also show that the DVO is *only* equal to $\frac{N}{2}$ for the ML detector for when $n = 2$.

- We propose three low-complexity antenna selection strategies: (i) the *max-norm* strategy selecting the antenna based on the maximum channel magnitude, (ii) the *min-phase* strategy selecting the antenna based on the minimum absolute channel angle, and (iii) the *max-distance* strategy selecting the antenna based on the distances to the decision boundary. We analytically characterize the symbol error probability (SEP) performance of all three strategies for the QPSK modulation under Rayleigh fading. These results are presented in Lemmas 1, 2 and 3.
- In order to characterize the reliability performance of the proposed antenna selection strategies in the high SNR regime, we also establish the DVO results for these strategies. We show that the max-norm DVO is equal to $\frac{1}{2}$ when $n = 2$, and to N when $n \geq 3$ for all $N \geq 1$ (Theorem 2). We show that the min-phase strategy can achieve the DVO 1 when $n = 2$, which presents a DVO improvement of 0.5 at this value of n when compared to the max-norm strategy (Theorem 3). However, the DVO of the min-phase strategy stays constant at 1 for $n \geq 3$. We show that the max-distance strategy enjoys the benefits of both max-norm and min-phase strategies, achieving the same DVO with the min-phase one at $n = 2$ and $N = 1, 2$, *whilst* achieving the full-DVO N for $n \geq 3$ (Theorem 4).

B. Related Work

The design of efficient signal detectors is an important and growing research area for low-resolution ADC based communication systems [12]. The conventional approaches such as those in [13]–[17] cannot be directly used when the detector is presented with coarsely quantized versions of signals. As an extension of conventional techniques, an optimal ML detector is presented in [11] for 1-bit ADC based wireless systems, where the transmitter is equipped with multiple antennas. The ML detector complexity grows exponentially with high signal constellations, the number of transmit antennas and the number of users in the uplink. To overcome this problem, [11] also presents a low-complexity zero-forcing receiver, which is simple to implement and shows comparable performance with the ML receiver in the low SNR regime. However, it experiences an error floor when SNR is high. The authors in [18] present a near maximum likelihood (nML) detector, which is based on convex optimization techniques. The nML detector gives better performance than the ZF-type detector for all SNR regimes. In the current paper, we generalize the ML detector presented in [11] to multi-bit phase quantization.

In [19], a sub-optimum detector named naive-ML is presented for a MIMO system and it shows almost the same performance as the optimum ML detector in the high SNR regime in terms of bit error rate (BER). In [20], the authors present another low-complexity nML detector called one-bit sphere decoding (OSD), for the uplink of a MIMO system equipped with 1-bit ADCs. The detection algorithm estimates the transmitted symbol vector sent by uplink users by searching over a sphere, which contains a collection of codeword vectors close to the received signal vector at the base station in terms of the weighted Hamming distance. The authors discuss the trade-off between performance and complexity with the dimension of the sphere and the length of the sub-vectors. A novel iterative detection and decoding scheme for uplink large-scale multiuser multiple-antenna systems based on 1-bit ADCs is presented in [21], where the authors propose a linear low-resolution-aware minimum mean square error detector for soft multiuser interference mitigation which can improve the bit error rate performance after several iterations. In [22], the authors focus on the development of soft-output detection methods for low-resolution ADCs and propose another near-optimal detector for a coded mm-wave MIMO system.

In [23], the authors propose a linear minimum mean square error (LMMSE) receiver when in-phase and quadrature components of the received signal are independently quantized by using a low-resolution ADC. They provide an approximation for the mean square error between transmitted and received symbols, and derive an optimized linear receiver that performs better than the conventional Wiener filter. Results in [23] are further extended to an iterative decision feedback receiver with quantized observations in [24]. More recently, there is progress in machine learning-based detection approaches as well [4], [25], [26]. In [4], [25] a reinforcement learning-based approach is used to design a robust likelihood function learning method for MIMO systems with 1-bit ADCs. For a similar system, a semi-supervised learning detector is proposed in [26], which can be further improved to an online-learning detector.

It is also an important and growing research area to analyze the performance of low-resolution ADC based wireless systems when compared to the traditional high-resolution quantization based ones. To this end, the link capacity with 1-bit ADCs under the additive quantization noise model (AQNM) is investigated in [1], [5], [27]. For multi-bit low-resolution ADCs, the capacity is also investigated in [3], which turns out to be a hard problem to obtain general capacity expressions. In [28], the authors present some bounds on the link capacity in the high SNR regime for multi-antenna systems with 1-bit ADCs under flat fading. The results characterize how the number of antennas impacts the capacity in the high SNR regime. Further, it is also shown in this paper that the capacity in the high SNR regime is lower bounded by the rank of the channel. The work in [28] is further extended in [27] to obtain a closed-form expression for multiple-input-single-output (MISO) channel capacity assuming that the channel state information is available both at the transmitter and receiver. Mutual information between the channel input and the quantized channel output of a 1-bit ADC based MIMO system is obtained in [29] and [30]. Using a second-order expansion of the mutual information function, it is shown in this work that the power penalty due to 1-bit quantization is approximately equal to $\frac{\pi}{2}\,(1.98\text{ dB})$. This confirms that

This article has been accepted for publication in a future issue of this journal, but has not been fully edited. Content may change prior to final publication. Citation information: DOI 10.1109/OJCOMS.2021.3133526, IEEE Open Journal of the Communications Society

low-resolution quantization performs adequately in the low SNR regime while reducing power consumption. In [31], the achievable downlink rate of a massive MIMO system with 1-bit ADCs is analyzed. The results show that it is enough to have approximately 2.5 times more antennas at the base station to overcome the loss due to 1-bit ADCs.

The use of low-resolution phase quantization has also been studied in recent years [7]–[9]. Numerical results in [32] show that a phase-quantized block non-coherent channel with 8-bit phase quantization under the QPSK modulation can recover about 80-85 percent of mutual information attained with unquantized observations when there is an extra 2-3 dB SNR gain. In [9], it is shown that a rotated 2^n-phase shift keying scheme is the capacity-achieving input distribution for a complex AWGN channel with n-bit phase quantization.

The material in this paper was presented in part in [33], where we focus only on the situation in which in-phase and quadrature channels are independently quantized using 1-bit ADCs under QPSK modulation with Rayleigh fading. The present paper expands upon the results presented in [33] and provides a rigorous error probability performance and DVO analysis with n-bit phase quantization. Theorem 1 of this paper presents the ML detection rule. Our analytical results in Theorems 2-5 along with the numerical ones presented in Section VI establish a fundamental asymptotic reliability characterization for low-resolution ADC based SIMO wireless systems in the high SNR regime. These results do not appear in our previous work [33], nor do they exist in any other previous paper in the literature.

C. Notation

We use uppercase letters to represent random variables, calligraphic letters to represent sets and bold letters to represent vectors. We use $\mathbb{R}$, $\mathbb{R}^2$ and $\mathbb{N}$ to denote the real line, 2-dimensional Euclidean space and natural numbers, respectively. For a pair of integers $i \leq j$, we use $[i:j]$ to denote the discrete interval $\{i, i+1, \ldots, j\}$. For two functions f and g, we will say $f(x) = O(g(x))$ as $x \to x_0$ if $|f(x)| \leq c\,|g(x)|$ for some $c > 0$ when x is sufficiently close to x_0. Similarly, we will say $f(x) = \Omega(g(x))$ as $x \to x_0$ if $|f(x)| \geq c\,|g(x)|$ for some $c > 0$ when x is sufficiently close to x_0. We write $f(x) = \Theta(g(x))$ as $x \to x_0$ if $f(x) = O(g(x))$ and $f(x) = \Omega(g(x))$ as $x \to x_0$. Finally, we will say $f(x) = o(g(x))$ as $x \to x_0$ if $\lim_{x \to x_0} \left|\frac{f(x)}{g(x)}\right| = 0$.

The set of complex numbers $\mathbb{C}$ is $\mathbb{R}^2$ equipped with the usual complex addition and complex multiplication. We write $z = z_{\rm re} + \jmath z_{\rm im}$ to represent a complex number $z \in \mathbb{C}$, where $\jmath = \sqrt{-1}$ is the imaginary unit of $\mathbb{C}$, and $z_{\rm re}$ and $z_{\rm im}$ are called, respectively, *real* and *imaginary* parts of z [34]. Every $z \in \mathbb{C}$ has also a *polar* representation $z = |z|\,e^{\jmath\theta} = |z|\,(\cos(\theta) + \jmath \sin(\theta))$, where $|z| \triangleq \sqrt{z_{\rm re}^2 + z_{\rm im}^2}$ is the magnitude of z and $\theta = \mathsf{Arg}(z) \in [-\pi, \pi)$ is called the (principle) argument of z. As is common in the communication and signal processing literature, $\mathsf{Arg}(z)$ will also be called the phase of z (modulo 2π). For a complex random variable $Z = Z_{\rm re} + \jmath Z_{\rm im}$, we define its mean and variance as $\mathsf{E}[Z] \triangleq \mathsf{E}[Z_{\rm re}] + \jmath \mathsf{E}[Z_{\rm im}]$ and $\mathsf{Var}(Z) \triangleq \mathsf{E}\left[|Z - \mathsf{E}[Z]|^2\right]$, respectively. We say that Z is *circularly-symmetric* if Z and $e^{\jmath\theta} Z$ induce the same probability distribution over $\mathbb{C}$ for all $\theta \in \mathbb{R}$ [35], [36]. For $x > 0$, $\log x$ and $\log_2 x$ will denote natural logarithm of x and logarithm of x in base 2, respectively.

II. System Setup

A. Channel Model and Signal Modulation

We consider a wireless channel consisting of a transmitter with one antenna and a receiver with N antennas for $N \geq 1$. The received signals at the receiver antenna array can be given in vector form as

$$\boldsymbol{Y} = \sqrt{\mathsf{SNR}}\boldsymbol{H}X + \boldsymbol{W}, \tag{1}$$

where $X \in \mathcal{C}$ is the transmitted signal with $\mathcal{C}$ denoting the signal constellation in $\mathbb{C}$, SNR is the ratio of the transmitted signal power to the AWGN power, $\boldsymbol{H} = [H_0 \quad H_1 \quad \cdots \quad H_{N-1}]^T$ with $H_l \in \mathbb{C}$ is the unit power channel gain between the transmitter and the l-th receiver antenna, and $\boldsymbol{W} = [W_0 \quad W_1 \quad \cdots \quad W_{N-1}]^T$ with W_l being the circularly-symmetric zero-mean unit-variance AWGN, i.e., $W_l \sim \mathcal{CN}(0,1)$, at the l-th receiver antenna. We will assume that the transmitted symbols are QPSK modulated, and take the set $\mathcal{C}$ as $\mathcal{C} = \left\{e^{\jmath\pi\left(\frac{2i+1}{4}-1\right)}\right\}_{i=0}^{3}$. For the system setup given in (1), under high-resolution quantization where the receiver can fully observe $\boldsymbol{Y} = \boldsymbol{y}$ with perfect channel knowledge $\boldsymbol{H} = \boldsymbol{h}$, the ML detector rule can be given as

$$\hat{x}_{\mathsf{high}}(\boldsymbol{y}, \boldsymbol{h}) = \arg\min_{x \in \mathcal{C}} \left\|\boldsymbol{y} - \sqrt{\mathsf{SNR}}\boldsymbol{h}x\right\|_2^2, \tag{2}$$

where $\|(\cdot)\|_2$ represents the Euclidean norm of the vector $(\cdot)$ [37]. In the present paper, on the other hand, we focus on the case where the receiver quantizes each incoming signal and conveys the quantized received signal vector $Q(\boldsymbol{Y}) = [Q(Y_0), Q(Y_1), \cdots, Q(Y_{N-1})]^T$ to the detector. By using these quantized observations, the detector has to estimate the transmitted signal X. Hence, there is no direct generalization of (2) to the low-resolution ADC based signal detection.

B. Receiver Architecture

The receiver architecture we consider is based on a low-resolution ADC in which the signal Y_l received from antenna l goes through an n-bit phase quantizer for all $l = 0, 1, \cdots, N-1$ as illustrated in Fig. 1. Then, the resulting quantized received signals are used to determine the transmitted symbol X. In this case, the quantizer $Q(\cdot)$ divides the complex domain $\mathbb{C}$ into 2^n quantization regions and outputs the index of the region in which Y_l lies as an input to the detector. More formally, we declare $Q(Y_l) = k$ if $Y_l \in \mathcal{R}_k$ for $k \in [0 : 2^n - 1]$, where $\mathcal{R}_k \subseteq \mathbb{C}$ is the k-th quantization region. Since information is encoded in the phase of X with the above choice of constellation points in our setup, we choose $\mathcal{R}_k$ as the convex cone given by

$$\mathcal{R}_k = \left\{z \in \mathbb{C} : \frac{2\pi}{2^n}k \leq \mathsf{Arg}(z) + \pi < \frac{2\pi}{2^n}(k+1)\right\}.$$

This article has been accepted for publication in a future issue of this journal, but has not been fully edited. Content may change prior to final publication. Citation information: DOI 10.1109/OJCOMS.2021.3133526, IEEE Open Journal of the Communications Society

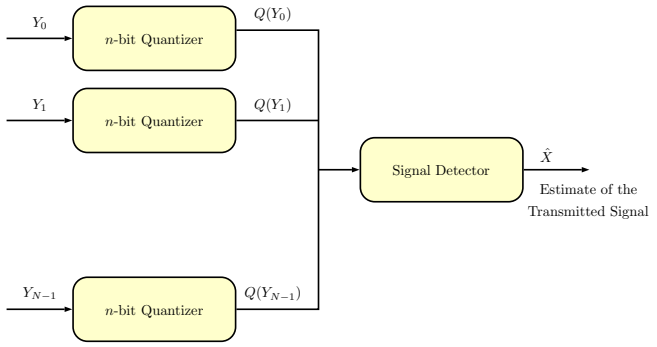

Figure 1: The receiver architecture with low-resolution quantization. The signal detector observes only the n-bit quantized versions of Y_l to estimate the transmitted signal. $l = 0, 1, \cdots N-1$

The use of phase quantization in our receiver architecture is motivated by the following factors. First, considering channel impairments as phase rotations in transmitted signals, quantization and decision regions for phase modulation are conveniently modelled as convex cones in the complex plane [38] as described above, without requiring the use of automatic gain control. In general, phase modulation is historically known to be optimum up to modulation order 16 under peak power limitations [39] and it is indeed the optimum modulation scheme for achieving the channel capacity with phase quantized outputs [40]. Second, phase quantizers can be implemented using one-bit ADCs that consist of simple comparators, and they consume negligible power (in the order of milliwatts). As given in [41], the implementation based on time-to-digital converters (TDCs) can also be adopted to further reduce the area and power consumption of the phase quantizer. On the other hand, phase modulation has an important and practical layering feature enabling the quantizer and detector design separation in low-resolution ADC based communications. For a given number of bits, the phase quantizer needs to be designed only once, and can be kept constant for all channel realizations. Therefore, the detector can be implemented digitally as a table look-up procedure using channel knowledge and quantizer output [7].

We also assume that full channel state information (CSI) is available at the receiver. Similar to our previous work in [8], the motivation behind our model with full-precision CSI is two-fold. First, in [42], it was shown that it is possible to attain a high channel estimation precision with the use of low-resolution ADCs by increasing the number of training symbols in the closed-loop estimation process. For example, it was shown in [42] that for $\mathsf{SNR} = 10$ dB, the estimator based on 3-bit ADC gives a mean square error of -20 dB with only 11 training symbols. Second, the mixed-ADC architectures are also commonly investigated in the literature, and they can be employed to achieve high channel estimation accuracy [43]. In a mixed-ADC architecture, high-resolution ADCs (structured through either serial or parallel connections) are used during the channel estimation stage [42]–[44] and during the data transmission phase, the receiver switches to low-resolution operation by using fewer quantization bits. Although the energy consumption is increased in this approach, this is not a restrictive degradation for our purposes. Each fading state will span a large group of information bits at the target multiple Gbits per second data rates in next-generation wireless systems. Hence, the energy saving during data transmission is more significant than the increased energy consumption during channel estimation. Based on the existing results for channel estimation accuracy with low-resolution quantizers, the assumption on the availability of full CSI at the receiver is also commonly used by many previous works in the field [45]–[47].

III. Optimum Signal Detection

The optimum maximum a posteriori (MAP) detector in our setup aims to minimize the SEP by using the knowledge of $Q(\boldsymbol{Y})$ and channel state information $\boldsymbol{H}$, which can be represented as selecting a signal point $\hat{x}(\boldsymbol{k}, \boldsymbol{h})$ satisfying

$$\hat{x}(\boldsymbol{k}, \boldsymbol{h}) = \underset{x \in \mathcal{C}}{\arg\max}\ \mathsf{Pr}\left\{X = x \middle| Q(\boldsymbol{Y}) = \boldsymbol{k}, \boldsymbol{H} = \boldsymbol{h}\right\}, \quad (3)$$

where $\boldsymbol{k} = [k_0, k_1, \cdots, k_{N-1}]^T$ with $Q(Y_l) = k_l$ and $\boldsymbol{h} = [h_0, h_1, \cdots, h_{N-1}]^T$ with $h_l \in \mathbb{C}$ for all $l \in [0 : N-1]$ and $k_l \in [0 : 2^n - 1]$. The main performance figure of merit for our detection problem is the average SEP given by

$$p(\mathsf{SNR}) = \mathsf{Pr}\left\{X \neq \hat{x}\left(Q(\boldsymbol{Y}), \boldsymbol{H}\right)\right\}. \quad (4)$$

For uniformly distributed transmit symbols, the MAP detector becomes equivalent to the ML detector, and therefore we will only focus on the ML detection rule for the rest of the paper. The ML detection rule for the above mentioned system setup with n-bit quantization is presented in the following theorem.

Theorem 1: Assume H_l has a continuous probability density function (pdf) for all $l = 0, 1, \cdots, N-1$ and $\mathcal{Q}(\cdot)$ is the complementary distribution function of the standard normal random variable. Then, $\hat{x}(\boldsymbol{k}, \boldsymbol{H})$ is unique with probability one and the ML detection rule for low-resolution ADC based receiver architecture with n-bit quantization can be given as

$$\hat{x}(\boldsymbol{k}, \boldsymbol{h}) = \underset{x \in \mathcal{C}}{\arg\max} \prod_{l=0}^{N-1} \left(\frac{1}{2^n} \exp\left(-\mathsf{SNR} r_l^2\right) + g\left(\mathsf{Arg}(x), k_l, h_l\right) \right), \quad (5)$$

where $g(\mathsf{Arg}(x), k_l, h_l)$ is given by (6).

Proof: See Appendix A. ∎

For the special case of 2-bit quantization, we can simplify the expression in (5) to (7), where $\mathsf{sgn}(\cdot)$ is the signum function.

IV. Antenna Selection Approach and Signal Detection

The computation of the likelihood function of the ML detector given in Theorem 1 involves the evaluation of numerical integrals in (6). This is likely to be an onerous task to carry out in real-time over each symbol period, especially for large values of N at high transmission rates. A promising alternative to the ML signal detection is the antenna selection

This article has been accepted for publication in a future issue of this journal, but has not been fully edited. Content may change prior to final publication. Citation information: DOI 10.1109/OJCOMS.2021.3133526, IEEE Open Journal of the Communications Society

$$g\left(\mathsf{Arg}\left(x\right),k_l,h_l\right)=\sqrt{\frac{\mathsf{SNR}}{\pi}}r_l\int_{k_l\frac{\pi}{2^{n-1}}}^{(k_l+1)\frac{\pi}{2^{n-1}}}\Big[\exp\left\{-\mathsf{SNR}r_l^2\sin^2\left(\alpha-\mathsf{Arg}\left(h_l\right)-\mathsf{Arg}\left(x\right)\right)\right\}$$
$$\cos\left(\alpha-\mathsf{Arg}\left(h_l\right)-\mathsf{Arg}\left(x\right)\right)\mathcal{Q}\left(-\sqrt{2\mathsf{SNR}}r_l\cos\left(\alpha-\mathsf{Arg}\left(h_l\right)-\mathsf{Arg}\left(x\right)\right)\right)\Big]d\alpha, \tag{6}$$

where $r_l=|h_1|$ is the magnitude of h_l, $\mathsf{Arg}\left(h_l\right)$ is the phase angle of h_l and $k_l=Q\left(Y_l\right)$.

$$\hat{x}\left(\boldsymbol{k},\boldsymbol{h}\right)=\arg\max_{x\in\mathcal{C}}\prod_{l=0}^{N-1}\mathcal{Q}\left(-\mathsf{sgn}\left(\mathsf{Re}\left(Y_l\right)\right)\sqrt{\mathsf{SNR}}r_l\cos\left\{\mathsf{Arg}\left(h_l\right)+\mathsf{Arg}\left(x\right)\right\}\right)$$
$$\mathcal{Q}\left(-\mathsf{sgn}\left(\mathsf{Im}\left(Y_l\right)\right)\sqrt{\mathsf{SNR}}r_l\sin\left\{\mathsf{Arg}\left(h_l\right)+\mathsf{Arg}\left(x\right)\right\}\right), \tag{7}$$

approach, where we first select an antenna that will give us a favourable diversity branch based on the observed channel states, and then use the single antenna ML detector to estimate the transmitted symbols over the selected antenna. The single antenna ML detector, unlike the multi-antenna one given in Theorem 1, is a simple low-complexity distance calculator [8]. We illustrate the antenna selection approach in Fig. 2 pictorially, and will further discuss its advantages over the ML signal detection in Section VII after establishing fundamental optimality properties and studying system performance in Sections V and VI.

In this section, we will propose three antenna selection strategies to reduce implementation complexity. The proposed strategies will be sub-optimum when compared to the high-complexity ML signal detection, yet they will still have provable asymptotically optimum SEP decay exponents in the high SNR regime.

More generally, in the antenna selection based signal detection approach, we first pick an antenna $L^\star$ according to a given selection strategy based on the observed channel states. The antenna selection rule in our setup can be defined formally as follows.

Definition 1: An antenna selection rule s is a mapping

$$s:\mathbb{C}^N\to\left[0:N-1\right], \tag{8}$$

which takes N fading coefficients as input and outputs the index of the selected antenna.

Once the antenna $L^\star$ is selected, the detector only uses the information available at antenna $L^\star$ to detect the transmitted signal. Thus, the optimum detector has to minimize the SEP using the knowledge of $Q\left(Y_{L^\star}\right)$ and $H_{L^\star}$, which can be represented as selecting a signal point $\hat{x}\left(k^\star,h^\star\right)$ satisfying

$$\hat{x}\left(k^\star,h^\star\right)\in\arg\max_{x\in\mathcal{C}}\ \mathsf{Pr}\left\{X=x\middle|Q(Y_{L^\star})=k^\star,H_{L^\star}=h^\star\right\},$$

for all $h^\star\in\mathbb{C}$ and $k^\star\in[0:2^n-1]$. After selecting an antenna, the SIMO system considered in Section II reduces to a point-to-point SISO system. Therefore, the ML detection rule under a given selection strategy can be given as

$$\hat{x}\left(k^\star,h^\star\right)=\arg\min_{x\in\mathcal{C}}\ \mathsf{dist}\left(\sqrt{\mathsf{SNR}}h^\star x,\mathcal{H}_{k^\star}\right), \tag{9}$$

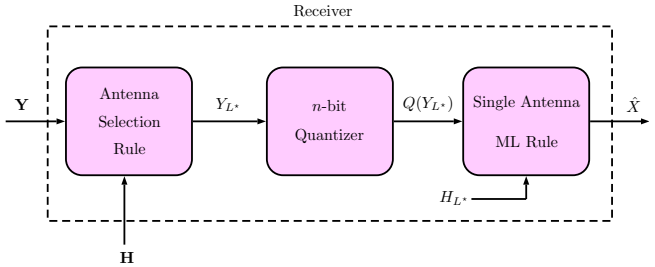

Figure 2: The antenna selection based low-resolution quantization receiver.

where $\mathsf{dist}\left(z,\mathcal{A}\right)\triangleq\inf_{s\in\mathcal{A}}|z-s|$ is the distance between a point $z\in\mathbb{C}$ and a set $\mathcal{A}\subseteq\mathbb{C}$, and $\mathcal{H}_{k^\star}=\left\{z\in\mathbb{C}:\mathsf{Arg}\left(z\right)+\pi=\frac{\pi}{2^n}\left(2k^\star+1\right)\right\}$ is the bisector of $\mathcal{R}_{k^\star}$ with $Y_{L^\star}\in\mathcal{R}_{k^\star}$ [8].

This discussion makes the role of a given antenna selection strategy and a separation principle clear in our setup. An antenna selection strategy does not interfere with the operation of the single antenna ML rule on the selected diversity branch, implying a layering architecture for receiver design where antenna selection and signal detection lie on different layers. Rather, it modifies the effective channel distribution (possibly favourably) to improve the SEP performance in the signal detection layer when averaged over the resulting fading channel distribution. Our SEP and DVO analysis below will depend on this observation critically to characterize the system performance, where we will derive the distributions for the effective channel gains that are used by the single antenna ML detector to estimate the transmitted symbols.

A. Max-Norm Antenna Selection Strategy

In this antenna selection strategy, the antenna with the maximum channel magnitude is chosen. The antenna selection rule can then be formally written according to

$$L^\star=\arg\max_{l\in[0:N-1]}\ R_l, \tag{10}$$

where $R_l=|H_l|$ is the channel magnitude of antenna l. The main idea behind this selection strategy is to choose the antenna with the channel that achieves the highest SNR. This selection strategy does not take into account the phase of the channel when selecting the antenna $L^\star$. Albeit its simplicity, it

This article has been accepted for publication in a future issue of this journal, but has not been fully edited. Content may change prior to final publication. Citation information: DOI 10.1109/OJCOMS.2021.3133526, IEEE Open Journal of the Communications Society

has some certain asymptotic optimality properties in the high SNR regime, which will be formally established in Section V. After selecting the antenna $L^\star$, the observations available in the selected antenna is used in (9) to estimate the transmitted symbol $\hat{x}\left(k^\star, h^\star\right)$.

B. Min-Phase Antenna Selection Strategy

In this antenna selection strategy, the antenna having the minimum absolute phase angle is chosen. The min-phase antenna selection rule can be formally expressed as

$$L^\star = \underset{l\in[0:N-1]}{\arg\min} \ \left|\Theta_l\right|, \tag{11}$$

where $\Theta_l = \mathsf{Arg}\left(H_l\right)$ is the phase angle of the channel in antenna l. The main motivation behind this selection technique is to minimize the negative effects of channel rotation on the SEP performance since the data is phase encoded. This selection strategy is also motivated by Theorem 2 of [8] which establishes the structure of the optimum detector choosing the channel rotated signal points closest to the bisector of the quantization region the channel outputs land in. The observations available in the selected antenna $L^\star$ is used in (9) to estimate the transmitted symbol $\hat{x}\left(k^\star, h^\star\right)$.

C. Max-Distance Antenna Selection Strategy

In this antenna selection strategy, the antenna $L^\star$ that locates the rotated constellation points $\sqrt{\mathsf{SNR}}H_l x$, $x \in \mathcal{C}$, furthest away from the boundary of the corresponding decision regions are chosen. The derivation of the antenna selection rule, in this case, is more complicated than the previous two considered above. An important observation to derive the antenna selection rule, in this case, is to realize that the decision regions, and therefore the corresponding boundaries, rotate as the channel angles change. For the QPSK modulation, we can obtain the max-distance antenna selection rule as follows.

Due to symmetry in the problem, it is enough to focus on only one constellation point, which we will take as $x = \mathrm{e}^{\jmath\frac{\pi}{4}}$, to derive the max-distance antenna selection rule. Let $\mathcal{E} = \left\{z \in \mathbb{C} : 0 \le \mathsf{Arg}\left(z\right) < \frac{\pi}{2}\right\}$. It is shown in [8] that the single antenna ML decision region for this constellation point can be given as

$$\mathcal{E}_k = \exp\left(\jmath\left(k - 2^{n-1}\right)\frac{2\pi}{2^n}\right)\mathcal{E} \tag{12}$$

if $H \in \mathcal{D}_k$ for $k \in [0 : 2^n - 1]$, where

$$\mathcal{D}_0 = \left\{z \in \mathbb{C} : \pi - \frac{\pi}{2^n} \le \mathsf{Arg}\left(z\right) < \pi\right\} \bigcup \left\{z \in \mathbb{C} : -\pi \le \mathsf{Arg}\left(z\right) < \frac{\pi}{2^n} - \pi\right\}$$

and

$$\mathcal{D}_k = \left\{z \in \mathbb{C} : (2k-1)\frac{\pi}{2^n} \le \mathsf{Arg}\left(z\right) + \pi < (2k+1)\frac{\pi}{2^n}\right\}.$$

We use H to refer to a generic fading state above.

The decision regions and boundaries are illustrated in Fig. 3 for 2-bit and 3-bit quantization.

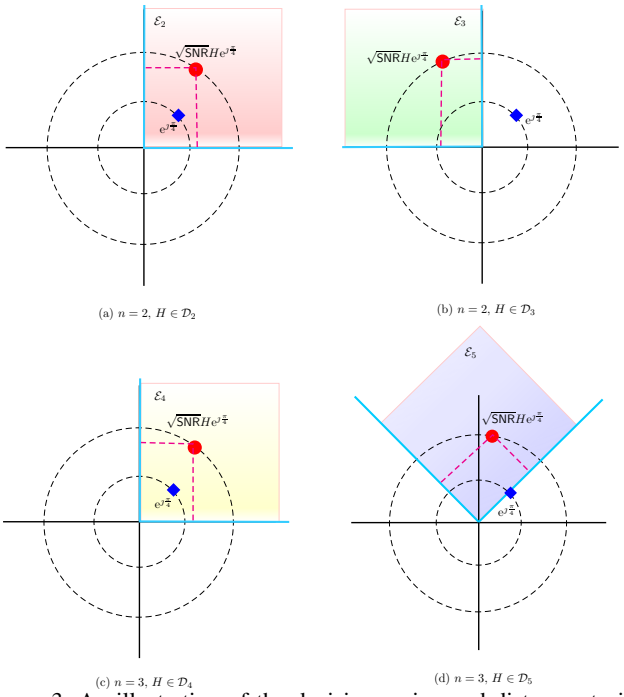

(a) $n = 2$, $H \in \mathcal{D}_2$ (b) $n = 2$, $H \in \mathcal{D}_3$ (c) $n = 3$, $H \in \mathcal{D}_4$ (d) $n = 3$, $H \in \mathcal{D}_5$

Figure 3: An illustration of the decision region and distances to its boundaries for QPSK modulation with 2-bit and 3-bit quantization. Original signal point $\mathrm{e}^{\jmath\frac{\pi}{4}}$ is indicated by '$\diamond$', whereas the rotated ones after multiplication with $\sqrt{\mathsf{SNR}}$ and H is indicated by '$\bullet$'. The decision regions are shaded areas and the boundaries are indicated by using solid blue lines.

By rotating the decision region in such a way that its boundary coincides with real and imaginary axes, the distance to the decision region boundary can be seen to be the minimum of $\left|\mathsf{Re}\left(\sqrt{\mathsf{SNR}}He^{\jmath\frac{\pi}{4}}\mathrm{e}^{-\jmath\left(K-2^{n-1}\right)\frac{2\pi}{2^n}}\right)\right|$ and $\left|\mathsf{Im}\left(\sqrt{\mathsf{SNR}}He^{\jmath\frac{\pi}{4}}\mathrm{e}^{-\jmath\left(K-2^{n-1}\right)\frac{2\pi}{2^n}}\right)\right|$, where $K = \sum_{k=0}^{2^n-1} k1_{\{H\in\mathcal{D}_k\}}$. Adapting these observations to the present antenna selection problem, we obtain (13) as the max-distance antenna selection rule.

A concept similar to the *max-distance* can be found in literature, especially used for precoding. In [48] and [49], the precoding techniques aim at minimizing the total multi-user interference such that the received signals lie as close as possible to the nominal constellation points are proposed. The optimization is based on maximizing the *safety margin* to the decision thresholds of the receiver constellation points. The safety margin separates the decision thresholds and the symbol region that is a downscaled version of the decision region. In this regard, the max-distance antenna selection strategy can be considered as the strategy selecting the antenna $L^\star$ with the maximum safety margin to the decision thresholds, using the terminology given in [48] and [49].

Finally, we note that there are alternative rotations to the one presented above in order to derive different versions of the antenna selection rule given in (13). For example, by considering a rotation of the decision region along with the rotated constellation point $\sqrt{\mathsf{SNR}}H_l x$, $x \in \mathcal{C}$, until the bisector of the decision region overlaps with the real axis, the distance from the rotated constellation point to the rotated

This article has been accepted for publication in a future issue of this journal, but has not been fully edited. Content may change prior to final publication. Citation information: DOI 10.1109/OJCOMS.2021.3133526, IEEE Open Journal of the Communications Society

$$L^\star = \underset{l\in[0:N-1]}{\arg\max}\ \min\left(\left|\mathsf{Re}\left(\sqrt{\mathsf{SNR}}H_l \mathrm{e}^{\jmath\frac{\pi}{4}}\mathrm{e}^{-\jmath\left(K_l-2^{n-1}\right)\frac{2\pi}{2^n}}\right)\right|, \left|\mathsf{Im}\left(\sqrt{\mathsf{SNR}}H_l \mathrm{e}^{\jmath\frac{\pi}{4}}\mathrm{e}^{-\jmath\left(K_l-2^{n-1}\right)\frac{2\pi}{2^n}}\right)\right|\right), \tag{13}$$

where $K_l = \sum_{k=0}^{2^n-1} k1_{\{H_l\in\mathcal{D}_k\}}$.

decision boundary can be expressed as

$$d_l = \mathsf{Re}\left(\sqrt{\mathsf{SNR}}H_l \mathrm{e}^{-\jmath\left(K_l-2^{n-1}\right)\frac{2\pi}{2^n}}\right) - \left|\mathsf{Im}\left(\sqrt{\mathsf{SNR}}H_l \mathrm{e}^{-\jmath\left(K_l-2^{n-1}\right)\frac{2\pi}{2^n}}\right)\right|,$$

where $K_l = \sum_{k=0}^{2^n-1} k1_{\{H_l\in\mathcal{D}_k\}}$. Further details on finding d_l can be found in [48]. d_l given above can be used to obtain another way to express the max-distance antenna selection rule (13). In the current paper, we will only focus on (13) to derive the SEP for the max-distance antenna selection strategy.

V. The Decay Exponent for the Average Symbol Error Probability

In this section, we will analyze the communication robustness that can be achieved with low-resolution ADCs by focusing on the decay exponent for $p(\mathsf{SNR})$, which is given by [1]

$$\mathsf{DVO} = -\lim_{\mathsf{SNR}\to\infty}\frac{\log p(\mathsf{SNR})}{\log \mathsf{SNR}}. \tag{14}$$

Following the convention in the field, we will call DVO the *diversity order*.

The following theorems will establish the DVO results for our system under the above antenna selection strategies as well as for the ML signal detection rule. To that end, we first derive the analytical expression for the SEP for each antenna selection strategy introduced in Section IV. We compare the SEP performances of the ML detector with all three selection strategies in Section VI.

A critical observation to derive the SEP performance of a selection strategy is that once the antenna $L^\star$ is selected, the setup reduces to a point-to-point system in which $H_{L^\star} = h^\star$ and $k_{L^\star} = k^\star$. To this end, with a slight abuse of notation, we define the SEP conditioned on the channel fading as

$$p(\mathsf{SNR}, h^\star) = \mathsf{Pr}\left\{\sqrt{\mathsf{SNR}}r^\star \mathrm{e}^{\jmath\theta^\star} + W^\star \notin \mathcal{E}^\star\right\}, \tag{15}$$

where $r^\star = |h^\star|$, $\theta^\star = \mathsf{Arg}(h^\star x)$, $W^\star$ is the noise on the selected antenna, which is still AWGN with the same mean and variance due to independence between noise and fading processes. The set $\mathcal{E}^\star$ is defined as $\mathcal{E}^\star = \left\{z\in\mathbb{C}: 0\le \mathsf{Arg}(z) < \frac{\pi}{2}\right\}$. The probability in (15) can be calculated by conditioning on the real part of $W^\star$, which is denoted by $W^\star_{\mathrm{re}}$ as,

$$\mathsf{Pr}\left\{\sqrt{\mathsf{SNR}}r^\star \mathrm{e}^{\jmath\theta^\star} + W^\star \notin \mathcal{E}^\star \,|\, W^\star_{\mathrm{re}} = w\right\} = \mathcal{Q}\left(\sqrt{2\mathsf{SNR}}r^\star\sin\theta^\star\right) \tag{16}$$

[1]We will show that the limit in (14) exists for the antenna selection strategies we study in the current paper. Hence, there is no ambiguity in the definition of DVO.

for $w \ge -\sqrt{\mathsf{SNR}}r^\star\cos\theta^\star$. Similarly, for $w < -\sqrt{\mathsf{SNR}}r^\star\cos\theta^\star$, we get

$$\mathsf{Pr}\left\{\sqrt{\mathsf{SNR}}r^\star \mathrm{e}^{\jmath\theta^\star} + W^\star \notin \mathcal{E}^\star \,\Big|\, W^\star_{\mathrm{re}} = w\right\} = 1. \tag{17}$$

Integrating (16) and (17) with respect to the pdf of $W^\star_{\mathrm{re}}$, which is given by $f_{W^\star_{\mathrm{re}}}(w) = \frac{1}{\sqrt{\pi}}\mathrm{e}^{-w^2}$, we obtain $p(\mathsf{SNR}, h^\star)$ as

$$p(\mathsf{SNR}, h^\star) = \mathcal{Q}\left(\sqrt{2\mathsf{SNR}}r^\star\cos\theta^\star\right) + \mathcal{Q}\left(\sqrt{2\mathsf{SNR}}r^\star\sin\theta^\star\right) - \mathcal{Q}\left(\sqrt{2\mathsf{SNR}}r^\star\cos\theta^\star\right)\mathcal{Q}\left(\sqrt{2\mathsf{SNR}}r^\star\sin\theta^\star\right). \tag{18}$$

Averaging $p(\mathsf{SNR}, H_{L^\star})$ with respect to the pdf of $H_{L^\star}$, we get the SEP expression for a given antenna selection strategy.

A. DVO with the Max-Norm Antenna Selection Strategy

To obtain the DVO under the max-norm antenna selection strategy given in Section IV-A, where the detector chooses the antenna $L^\star$ according to (10), we first obtain the average SEP which can be given as in Lemma 1.

Lemma 1: Consider a SIMO system with one transmit antenna and N receive antennas equipped with n-bit quantizers. Under max-norm antenna selection strategy, the average SEP with Rayleigh fading is given according to (19) where $p(\mathsf{SNR}, h^\star)$ is given in (18).

Proof: See Appendix B. ∎

In this case, using (19), the DVO can be obtained as in Theorem 2 below.

Theorem 2: Consider a SIMO system with one transmit antenna and N receive antennas equipped with n-bit quantizers. Under the max-norm antenna selection strategy, the DVO with QPSK modulation under Rayleigh fading is given according to

$$\mathsf{DVO} = \begin{cases} \frac{1}{2} & n = 2 \\ N & n \ge 3 \end{cases} \tag{20}$$

for all $N \ge 1$.

Proof: See Appendix C. ∎

B. DVO with the Min-Phase Antenna Selection Strategy

To obtain the DVO under the min-phase antenna selection strategy given in Section IV-B, where the detector chooses the antenna $L^\star$ according to (11), we first obtain the average SEP which can be given as in Lemma 2.

Lemma 2: Consider a SIMO system with one transmit antenna and N receive antennas equipped with n-bit quantizers. Under min-phase antenna selection strategy, the average SEP with Rayleigh fading is given according to (21), where $p(\mathsf{SNR}, h^\star)$ is given in (18).

Proof: See Appendix D. ∎

In this case, the DVO is given according to Theorem 3 below.

This article has been accepted for publication in a future issue of this journal, but has not been fully edited. Content may change prior to final publication. Citation information: DOI 10.1109/OJCOMS.2021.3133526, IEEE Open Journal of the Communications Society

$$p\left(\mathsf{SNR}\right)=\frac{2^{n}N}{\pi}\int_{\frac{\pi}{4}-\frac{\pi}{2^{n}}}^{\frac{\pi}{4}+\frac{\pi}{2^{n}}}\int_{0}^{\infty}p\left(\mathsf{SNR},h^{\star}\right)r^{\star}\exp\left\{-\left(r^{\star}\right)^{2}\right\}\left[1-\exp\left\{-\left(r^{\star}\right)^{2}\right\}\right]^{N-1}dr^{\star}\,d\theta^{\star}, \tag{19}$$

$$p\left(\mathsf{SNR}\right)=\frac{2^{n+1}N}{\pi}\int_{\frac{\pi}{4}}^{\frac{\pi}{4}+\frac{\pi}{2^{n}}}\int_{0}^{\infty}p\left(\mathsf{SNR},h^{\star}\right)r^{\star}\exp\left\{-\left(r^{\star}\right)^{2}\right\}\left(1+2^{n-2}-\frac{2^{n}\theta^{\star}}{\pi}\right)^{N-1}dr^{\star}\,d\theta^{\star}, \tag{21}$$

Theorem 3: Consider a SIMO system with one transmit antenna and N receive antennas equipped with n-bit quantizers. Under the min-phase antenna selection strategy, the DVO with QPSK modulation under Rayleigh fading is given according to

$$\mathsf{DVO}=\begin{cases}\frac{1}{2} & n=2 \text{ and } N=1\\ 1 & n\geq 3 \text{ and } N=1 \text{ or } n\geq 2 \text{ and } N\geq 2\end{cases}. \tag{22}$$

Proof: See Appendix E. ∎

C. DVO with the Max-Distance Antenna Selection Strategy

To obtain the DVO under the max-distance antenna selection strategy given in Section IV-C, where the detector chooses the antenna $L^{\star}$ according to (13), we first obtain the average SEP which can be given as in Lemma 3.

Lemma 3: Consider a SIMO system with one transmit antenna and N receive antennas equipped with n-bit quantizers. Under the max-distance antenna selection strategy, the average SEP with Rayleigh fading is given according to (23).

Proof: See Appendix F. ∎

Using Lemma 3, the DVO for the max-distance antenna selection strategy is given in the next theorem.

Theorem 4: Consider a SIMO system with one transmit antenna and N receive antennas equipped with n-bit quantizers. Under the max-distance antenna selection strategy, the DVO with QPSK modulation under Rayleigh fading is given according to

$$\mathsf{DVO}=\begin{cases}\frac{N}{2} & n=2 \text{ and } N\in\{1,2\}\\ N & n\geq 3 \text{ and } N\geq 1\end{cases}. \tag{24}$$

Proof: See Appendix G. ∎

We note that the proof of Theorem 4 for $n\geq 3$ directly follows from Theorem 2 since it gives us a lower bound for the max-distance DVO that matches with the high-resolution upper bound. Under the max-distance selection strategy, we are not able to completely characterize the DVO for all $N\geq 1$ and $n\geq 2$. The remaining case is the one where $n=2$ and $N\geq 3$. However, we conjecture that the DVO under the max-distance antenna selection strategy for this unresolved case is equal to $\frac{N}{2}$. This assertion is correct for the cases (i) $n=2$ and $N=1$ and (ii) $n=2$ and $N=2$, as indicated in Theorem 4. We also perform an extensive numerical study in Section VI to illustrate the DVO values achieved by the max-distance antenna selection strategy, which also verifies our conjecture.

D. DVO with the ML Signal Detection Rule

The analysis given above for the sub-optimum single antenna selection strategies has some important ramifications for characterizing the DVO achieved by the ML signal detection rule given in Theorem 1. In particular, the direct analysis of the SEP by using (5) does not lead to a tractable approach to discover the DVO for the optimum ML signal detection with low-resolution quantization and N receive antennas at the receiver.

However, Theorems 2 and 4 show that the DVO achieved by the max-norm and max-distance antenna selection strategies is equal to N for $n\geq 3$. This is a DVO lower bound on the performance of the ML detection rule since it always performs better than the max-norm and max-distance antenna selection strategies by its definition. On the other hand, it is well-known that the high-resolution DVO that can be achieved by using N antennas at the receiver is also equal to N [37]. These observations show that the DVO upper and lower bounds for the ML signal detection rule coincide with each other for $n\geq 3$, which establishes the DVO that can be achieved by the ML signal detection with multiple receive antennas and low-resolution quantization at the receiver for $n\geq 3$. This result is formally stated in the next theorem.

Theorem 5: Consider a SIMO system with one transmit antenna and N receive antennas equipped with n-bit quantizers. Under the ML detection rule given in Theorem 1, the DVO with QPSK modulation under Rayleigh fading is given according to

$$\mathsf{DVO}=\begin{cases}\frac{1}{2} & n=2 \text{ and } N=1\\ N & n\geq 3 \text{ and } N\geq 1\end{cases}. \tag{25}$$

It is important to note that Theorem 5 for $N=1$ directly follows from the results in [8]. The case for which we cannot characterize the DVO for the ML signal detection rule is the one in which $n=2$ and $N\geq 2$. As in the case of the max-distance antenna selection strategy, we conjecture that the DVO is equal to $\frac{N}{2}$ for the ML rule when $n=2$ and $N\geq 2$. This assertion holds for when $N=1$. Theorem 4 further shows that $\frac{N}{2}$ is a DVO lower bound for the ML rule for $n=2$ and $N=2$. The numerical results in the next section will illustrate these points in more detail, providing further numerical evidence for the conjecture.

VI. Numerical Results

In this section, we present analytical and simulated SEP results for QPSK modulation with n-bit phase quantization.

This article has been accepted for publication in a future issue of this journal, but has not been fully edited. Content may change prior to final publication. Citation information: DOI 10.1109/OJCOMS.2021.3133526, IEEE Open Journal of the Communications Society

$$p\left(\mathsf{SNR}\right)=\frac{2^{n+1}N}{\pi}\int_{\frac{\pi}{4}}^{\frac{\pi}{4}+\frac{\pi}{2^n}}\int_{0}^{\infty}p\left(\mathsf{SNR},h^{\star}\right)\left\{G\left(\sqrt{\mathsf{SNR}}r^{\star}\cos\theta^{\star}\right)\right\}^{N-1}r\exp\left\{-\left(r^{\star}\right)^{2}\right\}dr^{\star}\,d\theta^{\star} \tag{23}$$

where $p\left(\mathsf{SNR},h^{\star}\right)$ is given in (18) and

$$G\left(\sqrt{\mathsf{SNR}}r^{\star}\cos\theta^{\star}\right)=g\left(\sqrt{2}r^{\star}\cos\theta^{\star}\right)-2^{n-2}\left\{1-2\mathcal{Q}\left(\sqrt{2}r^{\star}\cos\theta^{\star}\right)\right\}^{2}$$

with $g\left(\alpha\right)=\frac{2^n}{\sqrt{\pi\mathsf{SNR}}}\int_0^{\alpha}\left\{1-2\mathcal{Q}\left(\frac{\sqrt{2}t}{\sqrt{\mathsf{SNR}}}\tan\left(\frac{\pi}{4}+\frac{\pi}{2^n}\right)\right)\right\}\exp\left(-\frac{t^2}{\mathsf{SNR}}\right)dt$. and $\mathcal{Q}\left(\cdot\right)$ is the complementary distribution function of the standard normal random variable [50].

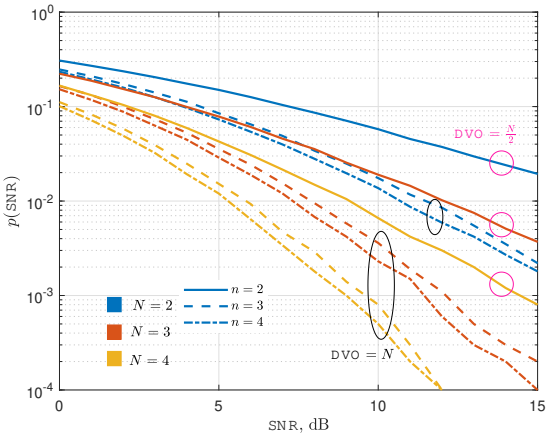

Figure 4: Average SEP curves as a function of SNR for QPSK modulation with ML detection. $n=2,3,4$ and $N=2,3,4$.

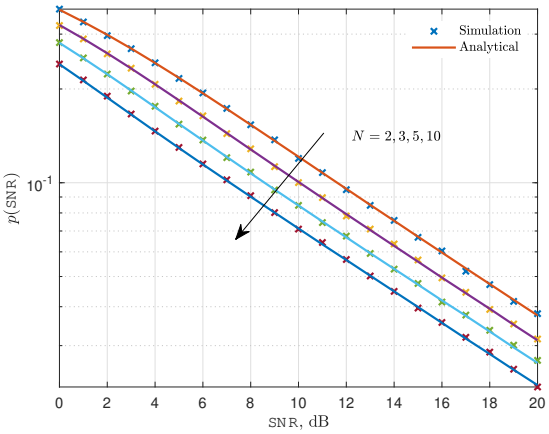

Figure 5: Average SEP curves as a function of SNR for QPSK modulation with the max-norm antenna selection strategy. $n=2$ and $N=2,3,5,10$.

Channel fading is unit-power with Rayleigh distributed magnitude, and additive noise is complex Gaussian with zero mean and unit variance.

A. System Performance with the ML Detector

First, we investigate the system performance with the optimum ML detector presented in Theorem 1. Fig. 4 plots the average SEP as a function of SNR for QPSK modulation with $n=2,3,4$-bit quantization under Rayleigh fading. We change the number of receive antennas as $N=2,3,4$ and simulate the SEP based on the detection rule provided in Theorem 1. We observe a noteworthy improvement in the average SEP when n changes from 2 to 3-bit quantization for QPSK modulation. By using the simulation results, we find that the DVO changes from $\frac{N}{2}$ to N when n changes from 2 to 3 or more, i.e., we observe full diversity order when the number of quantization bits is 3 as established in Theorem 5. This shows that using one extra bit, on top of 2 bits, improves SEP and DVO significantly. We also observe that the average SEP reduces as we increase n, but the amount by which it reduces also gets smaller as we increase n. This observation is a manifestation of the quantization invariance regime for $n\geq 3$ since the DVO stays constant at N for all values of n greater than or equal to 3.

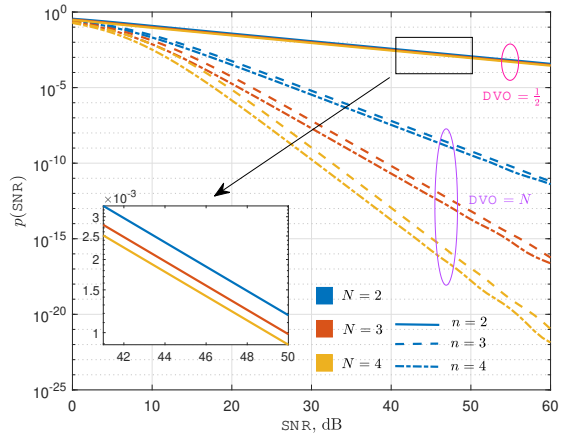

Figure 6: Average SEP curves as a function of SNR for QPSK modulation with the max-norm antenna selection strategy. $n=2,3,4$ and $N=2,3,4$.

B. System Performance under the Max-Norm Antenna Selection Strategy

Fig. 5 plots the average SEP as a function of SNR for QPSK modulation with $n=2$ bit quantization under Rayleigh fading. We change the number of receive antennas as $N=2,3,5,10$. The simulated results are generated using Monte Carlo simulation, while the analytical results are generated using our expression in (19). As the plot illustrates,

This article has been accepted for publication in a future issue of this journal, but has not been fully edited. Content may change prior to final publication. Citation information: DOI 10.1109/OJCOMS.2021.3133526, IEEE Open Journal of the Communications Society

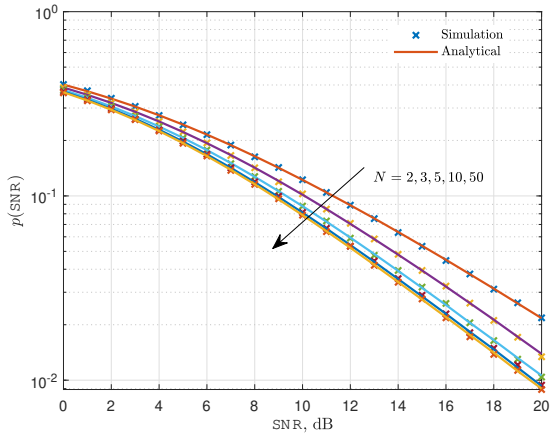

Figure 7: Average SEP curves as a function of SNR for QPSK modulation with min-phase antenna selection strategy. $n = 2$ and $N = 2, 3, 5, 10, 50$.

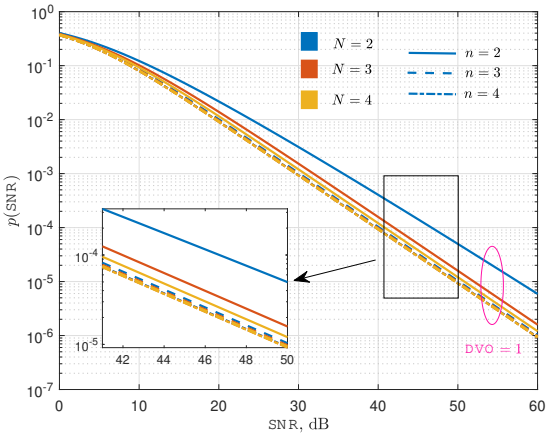

Figure 8: Average SEP curves as a function of SNR for QPSK modulation with min-phase antenna selection strategy. $n = 2, 3, 4$ and $N = 2, 3, 4$.

the analytical results accurately follow the simulated results for all four cases. As established in Theorem 2, we observe that with 2-bit quantization, the DVO remains $\frac{1}{2}$ for all N. We also observe that the average SEP reduces as we increase N, but the amount by which it reduces also gets smaller as we increase N.

Fig. 6 plots the average SEP as a function of SNR for QPSK modulation with $n = 2, 3, 4$ bit quantization under Rayleigh fading. We also change the number of antennas as $N = 2, 3, 4$. The plots are generated using the analytical expression in (19). The zoomed-in section of the plot illustrates the average SEP with 2-bit quantization more clearly. We observe a noteworthy improvement in the average SEP when n changes from 2 to 3- bit quantization for all $N = 2, 3, 4$. For example, when we fix the SNR at 20 dB and 45 dB for $N = 2$, we observe an average SEP improvement of approximately 40 and 3×10^5 times, respectively by using 3 bits at the quantizer instead of 2 bits. This is expected in light of Theorem 2, which states that using one extra bit, on top of 2-bits, improves the DVO from $\frac{1}{2}$ to N. We also observe that the average SEP reduces as we increase n, but the amount by which it reduces also gets smaller as we increase n. As proven in Theorem 2, DVO $= N$ for all $n \geq 3$ and DVO $= \frac{1}{2}$ when $n = 2$, which is also verified by Fig 6.

C. System Performance under the Min-Phase Antenna Selection Strategy

Fig. 7 plots the average SEP as a function of SNR for QPSK modulation with $n = 2$ bit quantization under Rayleigh fading. We change the number of antennas as $N = 2, 3, 5, 10$. The simulated results are generated using Monte Carlo simulation, while the analytical results are generated using our expression in (21). As the plot illustrates, the analytical results accurately follow the simulated results for all cases. As established in Theorem 3, we observe that the DVO $= 1$ for $n = 2$ and $N \geq 2$. We also observe that the average SEP reduces as we increase N, but the amount by which it reduces also gets smaller as we increase N.

Fig. 8 plots the average SEP as a function of SNR for QPSK modulation with $n = 2, 3, 4$ bit quantization under Rayleigh fading. We also change the number of antennas as $N = 2, 3, 4$. The plots are generated using the analytical expression in (21). We do not observe a noteworthy improvement in the average SEP even when we use more quantization bits. For example, when we fix the SNR at 20 dB and 45 dB for $N = 2$, we observe an average SEP improvement of approximately 2 and 5 times, respectively by using 3 bits at the quantizer instead of 2 bits. This is expected in light of Theorem 3, which states that the DVO is 1 for all $n \geq 2$ and $N \geq 2$. We also observe that the average SEP reduces as we increase n, but the amount by which it reduces also gets smaller as we increase n.

D. System Performance under the Max-Distance Antenna Selection Strategy

Fig. 9 plots the average SEP as a function of SNR for QPSK modulation with $n = 2$ bit quantization under Rayleigh fading. We change the number of antennas as $N = 2, 3, 4$. The simulated results are generated using Monte Carlo simulation, while the analytical results are generated using our expression in (23) for $n = 2$. As the plot illustrates, the analytical results accurately follow the simulated results for all cases. We observe a noteworthy improvement in the average SEP when N changes. In all cases, Fig. 9 indicate that the DVO is equal to $\frac{N}{2}$ with 2-bit quantization. We note that this result has been formally established for $N = 2$ and $n = 2$ in Theorem 4.

Fig. 10 plots the average SEP as a function of SNR for QPSK modulation with $n = 2, 3, 4$-bit quantization under Rayleigh fading. We change the number of antennas as $N = 2, 3, 4$. The curves are generated using the analytical expression in (23) for $n \geq 3$. We observe a noteworthy improvement in the average SEP when n changes from 2 to 3-bit quantization for all $N = 2, 3, 4$. For example, when we fix the SNR at 20 dB and 45 dB for $N = 2$, we observe an average SEP improvement of approximately 17 and 6×10^3

This article has been accepted for publication in a future issue of this journal, but has not been fully edited. Content may change prior to final publication. Citation information: DOI 10.1109/OJCOMS.2021.3133526, IEEE Open Journal of the Communications Society

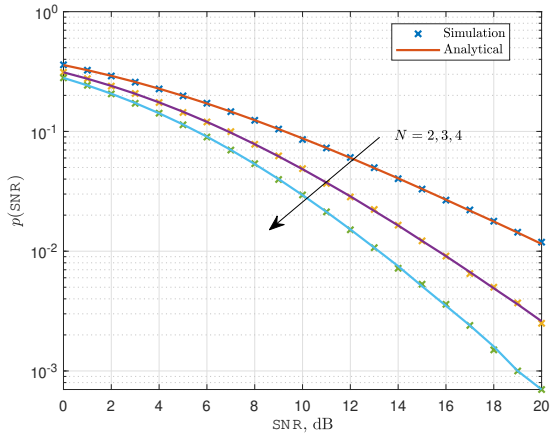

Figure 9: Average SEP curves as a function of SNR for QPSK modulation with the max-distance antenna selection strategy. $n = 2$ and $N = 2, 3, 4$.

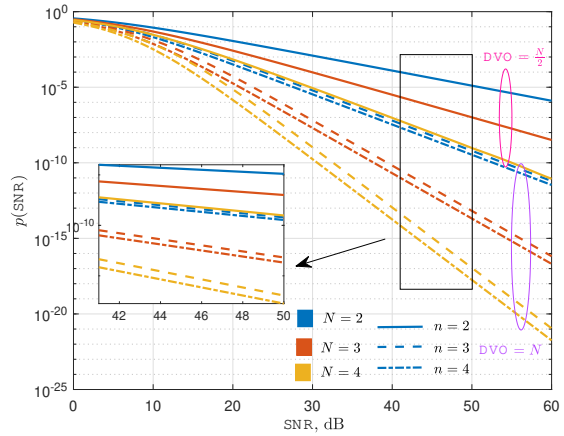

Figure 10: Average SEP curves as a function of SNR for QPSK modulation with the max-distance antenna selection strategy. $n = 2, 3, 4$ and $N = 2, 3, 4$.

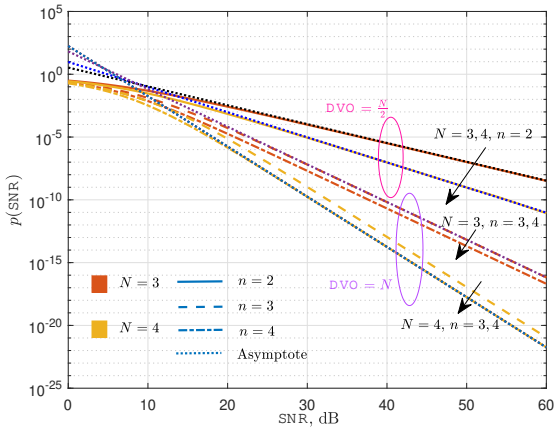

Figure 11: Asymptotic average SEP curves as a function of SNR for QPSK modulation with the max-distance antenna selection strategy $n = 2, 3, 4$ and $N = 3, 4$. For the clarity of the figure, we only illustrate the asymptotes for $N = 3, n = 2$, $N = 3, n = 3$, $N = 4, n = 2$ and $N = 4, n = 4$ cases.

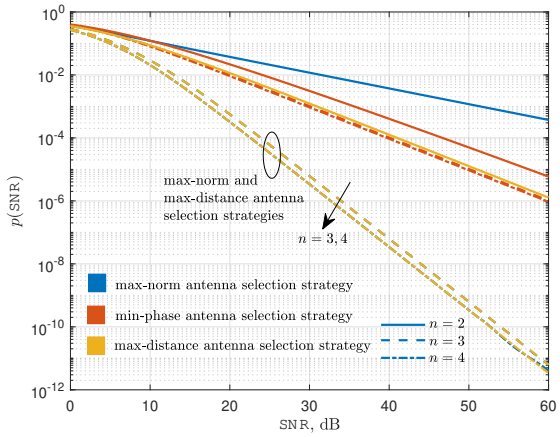

Figure 12: Average SEP curves as a function of SNR for QPSK modulation with different antenna selection strategies. $n = 2, 3, 4$ and $N = 2$.

times, respectively by using 3 bits at the quantizer instead of 2 bits. We also observe that the average SEP reduces as we increase n, but the amount by which it reduces also gets smaller as we increase n. Through numerical analysis, we can observe that using one extra bit, on top of 2-bits, improves the DVO from $\frac{N}{2}$ to N. To help with analysing the DVO numerically, we plot the asymptotic SEP curves as illustrated in Fig. 11. To that end, we observe that the DVO $= N$ for all $n \geq 3$ and DVO $= \frac{N}{2}$ when $n = 2$ which is in line with our formal DVO characterization for the max-distance antenna selection strategy established in Theorem 4.

E. System Performance Comparison

Fig. 12 plots the average SEP as a function of SNR for QPSK modulation under Rayleigh fading with the max-norm, min-phase and max-distance selection strategies with $n = 2, 3, 4$ and $N = 2$. The curves are generated using our analytical expressions in (19), (21) and (23) for the max-norm, min-phase and max-distance selection strategies, respectively.

We observe that the max-distance antenna selection strategy outperforms the other two antenna selection strategies in terms of average SEP for $n = 2$ with a notable SEP margin. For example, when we fix the SNR at 20 dB and 45 dB for $N = 2$ with $n = 2$, we observe an average SEP improvement of approximately 3 and 2 times, by employing the max-distance antenna selection strategy instead of the max-norm and min-phase antenna selection strategies, respectively. On the other hand, the max-norm antenna selection strategy performs almost similar to the max-distance antenna selection strategy when $n \geq 3$. This is an expected result since both strategies achieve the full DVO N for $n \geq 3$, i.e., see Theorems 2 and 4. In this case, the max-distance and the max-norm antenna selection strategy outperforms min-phase antenna selection strategy by a clear margin in terms of the average SEP since they can achieve much higher DVO values for $n \geq 3$, i.e., compare the analytical DVO results in Theorems 2-4.

Fig. 13 plots the average SEP as a function of SNR

This article has been accepted for publication in a future issue of this journal, but has not been fully edited. Content may change prior to final publication. Citation information: DOI 10.1109/OJCOMS.2021.3133526, IEEE Open Journal of the Communications Society

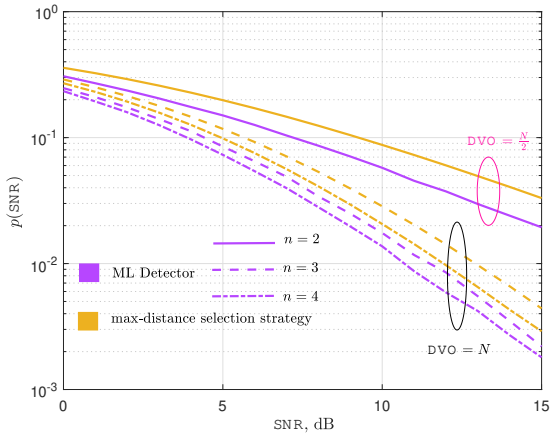

Figure 13: Average SEP curves as a function of SNR for QPSK modulation with the ML detector and max-distance antenna selection strategy. $n = 2, 3, 4$ and $N = 2$.

for QPSK modulation under Rayleigh fading with the ML detector and the max-distance antenna selection strategy with $n = 2, 3, 4$ and $N = 2$. The curves related to the ML detector are generated using Monte Carlo simulation and the curves related to the max-distance antenna selection strategy are generated using the analytical expression in (23). We observe that the max-distance antenna selection strategy shows the same DVO performance compared to the ML detector through our numerical analysis. That is, with 2-bit quantization the DVO is $\frac{N}{2}$ and with 3 or more bit quantization, the DVO is equal to N for both detection strategies, where the latter results have been formally obtained in Theorems 4 and 5.

VII. Discussion: System Design Guidelines

Our analysis in Section V (analytical) and Section VI (numerical) establishes fundamental reliability trends for SIMO channels with low-resolution quantization under Rayleigh fading. In this section, we provide a brief discussion on system design guidelines that can be gleaned from this analysis.

The ML detection rule given in Theorem 1 is the optimum signal detection strategy that outperforms the proposed max-norm, min-phase and max-distance antenna selection strategies. However, implementation of the ML rule depends on the computation of the likelihood function given in (5), which further necessitates the calculation of the integral expression in (6). This has to be done at each symbol period and for all constellation points to obtain the maximum likelihood estimator for the transmitted symbol. On the other hand, the proposed antenna selection strategies are much simpler to implement in real-time at the hardware level. For all antenna selection strategies, we first select an antenna before starting the signal detection phase. The antenna selection is a simple comparison operation among N antennas. After an antenna is selected for reception, we use the single antenna ML rule for detection, which is also a simple distance calculator, i.e., see [8]. While being less complex to implement, the proposed antenna selection strategies perform close to the ML rule with certain asymptotic optimality properties as established in Section V and numerically illustrated in Section VI. Hence, the antenna selection approach provides a low-complexity and high-performance design alternative for the optimum ML signal detection for SIMO low-resolution communication systems. [2]

From a system design point of view, another significant but less evident feature of the antenna selection approach is the utilization of the quantization bits. With antenna selection, we only require one n-bit quantizer to quantize and detect the transmitted symbols. The output of the selected antenna can be connected to the input of the quantizer for signal detection. In the ML signal detection rule, on the other hand, we jointly utilize all the antennas, where each is equipped with an n-bit quantizer. From this perspective, an antenna selection strategy has the potential of consuming N times less energy than the ML approach as well as simplifying the receiver design and reducing the form-factor. An open design problem, which we do not address in the current paper, is the jointly optimum bit allocation and signal detection problem using n quantization bits and N receive antennas. Given the already established optimality properties of the max-distance antenna selection strategy, we hypothesize that it would perform close to the solution of this joint optimization problem.

VIII. Conclusions and Future Generalizations

In this paper, we analyze the SEP performance of a low-resolution quantization based SIMO communication system. We present three antenna selection strategies and analytically characterize their SEP performance limits for QPSK modulation under Rayleigh fading. We establish that the max-distance antenna selection strategy, which selects the antenna based on distances to the decision boundaries, performs the same with the optimum ML signal detection rule in terms of the DVO (diversity order) metric. In particular, for both approaches, the decay exponent for the average SEP is equal to N when the number of quantization bits is equal to 3 or more, which is the full DVO that can be achieved by using infinite-bit quantizers. On the other hand, when the number of quantization bits is equal to 2, there is a significant reduction in diversity from N to $\frac{N}{2}$, as indicated by our numerical results and established analytically for some specific cases.

An interesting future extension of this work is the generalization of the proposed selection strategies to M-PSK modulation under Nakagami-m fading. This will allow generalizing our findings to broader cases. We also aim to extend the analysis in the paper to the cases where the transmitter also has multiple transmit antennas.

[2] In the current paper, we focus only on the slowly varying fading scenarios where the fading states stay constant for a large block of symbols. However, even in more rapidly varying fading situations where the antenna selection needs to be updated more frequently, the proposed approach provides a low-complexity signal detection framework when compared to the ML detection given in (5) since the single antenna ML rule is a simple distance calculator [8] and the antenna selection is also a low-complexity comparison operation.

This article has been accepted for publication in a future issue of this journal, but has not been fully edited. Content may change prior to final publication. Citation information: DOI 10.1109/OJCOMS.2021.3133526, IEEE Open Journal of the Communications Society

APPENDIX A
PROOF OF THEOREM 1

To obtain the ML detection rule, we have to maximize the likelihood function $\mathcal{L}(x)$ given by

$$\begin{aligned}\mathcal{L}(x) &= \mathsf{Pr}\left\{Q(\boldsymbol{Y}) = \boldsymbol{k} \,|\, X = x, \boldsymbol{H} = \boldsymbol{h}\right\}, \\ &= \prod_{l=0}^{N-1} \mathsf{Pr}\left\{\sqrt{\mathsf{SNR}} h_l x + W_l \in \mathcal{R}_{k_l} \,|\, X = x, H_l = h_l\right\}.\end{aligned} \tag{26}$$

In other words, we need to maximize the probability $\mathsf{Pr}\left\{Y_l \in \mathcal{R}_{k_l} \,|\, X = x, H_l = h_l\right\}$ and to that end, we first write the real and imaginary parts of the received signal Y_l at antenna l respectively as

$$\begin{aligned}Y_l^{\mathrm{re}} &= \sqrt{\mathsf{SNR}} r_l \cos\left(\theta_l + \theta_x\right) + W_l^{\mathrm{re}} \\ Y_l^{\mathrm{im}} &= \sqrt{\mathsf{SNR}} r_l \sin\left(\theta_l + \theta_x\right) + W_l^{\mathrm{im}},\end{aligned}$$

where $r_l = |h_l|$, $\theta_l = \mathsf{Arg}(h_l)$ and $\theta_x = \mathsf{Arg}(x)$. Since W_l^{re} and $W_l^{\mathrm{im}} \sim \mathcal{N}\left(0, \frac{1}{2}\right)$, given $H_l = h_l$ we have $Y_l^{\mathrm{re}} \sim \mathcal{N}\left(\sqrt{\mathsf{SNR}} r_l \cos\left(\theta_l + \theta_{\hat{x}}\right), \frac{1}{2}\right)$ and $Y_l^{\mathrm{im}} \sim \mathcal{N}\left(\sqrt{\mathsf{SNR}} r_l \sin\left(\theta_l + \theta_{\hat{x}}\right), \frac{1}{2}\right)$. Hence the joint pdf of Y_l^{re} and Y_l^{im} can be expressed as

$$\begin{aligned}f_{Y_l^{\mathrm{re}}, Y_l^{\mathrm{im}}}\left(y_l^{\mathrm{re}}, y_l^{\mathrm{im}}\right) = \\ \frac{1}{\pi} \exp\Big\{ &- \left(y_l^{\mathrm{re}} - \sqrt{\mathsf{SNR}} r_l \cos\left(\theta_l + \theta_x\right)\right)^2 \\ &- \left(y_l^{\mathrm{im}} - \sqrt{\mathsf{SNR}} r_l \sin\left(\theta_l + \theta_x\right)\right)^2 \Big\}.\end{aligned} \tag{27}$$

Thus, for each l we can find $\mathsf{Pr}\left\{Y_l \in \mathcal{R}_{k_l} \,|\, X = x, H_l = h_l\right\}$ by integrating the above pdf within appropriate regions. Since these regions are convex cones, to make our analysis easier we convert the pdf into polar coordinates as follows.

$$\begin{aligned}&\mathsf{Pr}\left\{Y_l \in \mathcal{R}_{k_l} \,|\, X = x, H_l = h_l\right\} = \\ &\int_{k_l \frac{\pi}{2^{n-1}}}^{(k_l+1)\frac{\pi}{2^{n-1}}} \int_0^{\infty} f_{Y_l^{\mathrm{re}}, Y_l^{\mathrm{im}}}\left(r\cos\theta, r\sin\theta\right) r \, dr \, d\theta.\end{aligned} \tag{28}$$

By substituting (27) into (28) and using the integral identity given by

$$\begin{aligned}\int z \exp\left(-az^2 + bz + c\right) dz \\ = \frac{\sqrt{\pi}}{4a^{\frac{3}{2}}} b \exp\left(c + \frac{b^2}{4a}\right) \mathrm{erf}\left(\frac{2az - b}{2\sqrt{a}}\right) \\ - \frac{1}{2a} \exp\left(-az^2 + bz + c\right) + C,\end{aligned}$$

where C is a constant, we can reduce this integral expression to

$$\begin{aligned}\mathsf{Pr}\left\{Y_l \in \mathcal{R}_{k_l} \,|\, X = x, H_l = h_l\right\} = \frac{1}{2^n} \exp\left(-\mathsf{SNR} r_l^2\right) \\ + \sqrt{\frac{\mathsf{SNR}}{\pi}} r_l \, g\left(\mathsf{Arg}(x), k_l, h_l\right),\end{aligned} \tag{29}$$

where $g\left(\mathsf{Arg}(x), k_l, h_l\right)$ is given in Theorem 1. Substituting (29) into (26), the ML detection rule given in (5) can be achieved.

APPENDIX B
PROOF OF LEMMA 1

We will first start with a definition that will simplify the notation below.

Definition 2: We say a function f is *exponentially equal* to SNR^d if $\lim_{\mathsf{SNR}\to\infty} \frac{\log f(\mathsf{SNR})}{\log \mathsf{SNR}} = d$ for some $d \in \mathbb{R}$. We write $f(\mathsf{SNR}) \overset{\mathrm{e}}{=} \mathsf{SNR}^d$ to indicate exponential equality whenever this limit exists. Similarly, we also write $f(\mathsf{SNR}) \overset{\mathrm{e}}{\leq} \mathsf{SNR}^d$ and $f(\mathsf{SNR}) \overset{\mathrm{e}}{\geq} \mathsf{SNR}^d$ if $\lim_{\mathsf{SNR}\to\infty} \frac{\log f(\mathsf{SNR})}{\log \mathsf{SNR}} \leq d$ and $\lim_{\mathsf{SNR}\to\infty} \frac{\log f(\mathsf{SNR})}{\log \mathsf{SNR}} \geq d$, respectively.

To start with the proof, we write the cdf of $R^\star = |H_{L^\star}|$ as

$$F_{R^\star}(r^\star) = \mathsf{Pr}\left\{R^\star \leq r^\star\right\} = \left[1 - \exp\left\{-\left(r^\star\right)^2\right\}\right]^N,$$

because the channel fading from the transmitter to each receiving antenna is independent. Therefore, the pdf of $R^\star$ can be given as

$$f_{R^\star}(r^\star) = 2Nr^\star \exp\left\{-\left(r^\star\right)^2\right\} \left[1 - \exp\left\{-\left(r^\star\right)^2\right\}\right]^{N-1}. \tag{30}$$

To complete the rest of the proof, we follow a similar analysis to the one given under the proof of Theorem 3 of our previous work in [8]. As such, $\theta^\star$ lies uniformly between $\left(\frac{\pi}{4} - \frac{\pi}{2^n}\right)$ and $\left(\frac{\pi}{4} + \frac{\pi}{2^n}\right)$ with n-bit quantization. Then, we get the expression in (19) by averaging (18) with respect to the pdfs of $R^\star$ and $\theta^\star$.

APPENDIX C
PROOF OF THEOREM 2

To start the proof, let us first define

$$\begin{aligned}p_1(\mathsf{SNR}) = \int_{\frac{\pi}{4}-\frac{\pi}{2^n}}^{\frac{\pi}{4}+\frac{\pi}{2^n}} \int_0^{\infty} \mathcal{Q}\left(\sqrt{2\mathsf{SNR}} r \cos\theta\right) r \exp\left(-r^2\right) \\ \left[1 - \exp\left(-r^2\right)\right]^{N-1} dr \, d\theta, \\ p_2(\mathsf{SNR}) = \int_{\frac{\pi}{4}-\frac{\pi}{2^n}}^{\frac{\pi}{4}+\frac{\pi}{2^n}} \int_0^{\infty} \mathcal{Q}\left(\sqrt{2\mathsf{SNR}} r \sin\theta\right) r \exp\left(-r^2\right) \\ \left[1 - \exp\left(-r^2\right)\right]^{N-1} dr \, d\theta, \\ p_3(\mathsf{SNR}) \\ = \int_{\frac{\pi}{4}-\frac{\pi}{2^n}}^{\frac{\pi}{4}+\frac{\pi}{2^n}} \int_0^{\infty} \mathcal{Q}\left(\sqrt{2\mathsf{SNR}} r \cos\theta\right) \mathcal{Q}\left(\sqrt{2\mathsf{SNR}} r \sin\theta\right) \\ r \exp\left(-r^2\right) \left[1 - \exp\left(-r^2\right)\right]^{N-1} dr \, d\theta.\end{aligned}$$

By using $\mathcal{Q}(x) = \frac{1}{\pi} \int_0^{\frac{\pi}{2}} \exp\left(-\frac{x^2}{2\sin^2\beta}\right) d\beta$ from the Craig's formula and $\left[1 - \exp\left(-r^2\right)\right]^{N-1} = \sum_{i=0}^{N-1} \binom{N-1}{i} \left((-1)^i \exp\left(-ir^2\right)\right)$ from the Binomial expansion, we can re-express $p_1(\mathsf{SNR})$ as

$$\begin{aligned}p_1(\mathsf{SNR}) = \int_0^{\frac{\pi}{2}} \int_{\frac{\pi}{4}-\frac{\pi}{2^n}}^{\frac{\pi}{4}+\frac{\pi}{2^n}} \int_0^{\infty} \sum_{i=0}^{N-1} \binom{N-1}{i} (-1)^i \\ r \exp\left\{-\left(i + 1 + \frac{\mathsf{SNR}\cos^2\theta}{\sin^2\beta}\right) r^2\right\} dr d\theta d\beta,\end{aligned}$$

This article has been accepted for publication in a future issue of this journal, but has not been fully edited. Content may change prior to final publication. Citation information: DOI 10.1109/OJCOMS.2021.3133526, IEEE Open Journal of the Communications Society

where $\binom{N-1}{i} = \frac{(N-1)!}{i!\,(N-1-i)!}$. We further can use [50, eq. 3.321] to reduce this integral to

$$p_1(\mathsf{SNR}) = \int_0^{\frac{\pi}{2}} \int_{\frac{\pi}{4}-\frac{\pi}{2^n}}^{\frac{\pi}{4}+\frac{\pi}{2^n}} \sum_{i=0}^{N-1} \binom{N-1}{i} (-1)^i \frac{\sin^2\beta}{2\left\{(i+1)\sin^2\beta + \mathsf{SNR}\cos^2\theta\right\}} d\theta d\beta.$$

After doing some mathematical manipulations using [50, eq. 2.562], we define $\rho_{\mathsf{SNR}}(\beta)$ which is a collection of functions indexed by SNR given as (31).

Hence, we can re-express $p_1(\mathsf{SNR})$ using $\rho_{\mathsf{SNR}}(\beta)$ as

$$p_1(\mathsf{SNR}) = \frac{1}{2}\int_0^{\frac{\pi}{2}} \sum_{i=0}^{N-1} \binom{N-1}{i} (-1)^i \sin^2\beta\, \rho_{\mathsf{SNR}}(\beta)\, d\beta.$$

We first analyze the above integral expression for $n = 2$ case. In this case, the numerator of $\rho_{\mathsf{SNR}}(\beta)$ equals to $\frac{\pi}{2}$ and $p_1(\mathsf{SNR})$ can be expressed as

$$p_1(\mathsf{SNR}) = \frac{\pi}{4}\int_0^{\frac{\pi}{2}} \sum_{i=0}^{N-1} \binom{N-1}{i} (-1)^i \frac{\sin^2\beta}{\sqrt{(i+1)\sin^2\beta\left\{(i+1)\sin^2\beta + \mathsf{SNR}\right\}}} d\beta.$$

$$= \mathsf{SNR}^{-\frac{1}{2}}\frac{\pi}{4}\int_0^{\frac{\pi}{2}} \sum_{i=0}^{N-1} \binom{N-1}{i} (-1)^i \frac{\sin^2\beta}{\sqrt{(i+1)\sin^2\beta\left\{\frac{(i+1)\sin^2\beta}{\mathsf{SNR}} + 1\right\}}} d\beta.$$

Therefore, we have $p_1(\mathsf{SNR}) = \mathsf{SNR}^{-\frac{1}{2}}\frac{\pi}{8}\sum_{i=0}^{N-1}\binom{N-1}{i}\frac{(-1)^i}{\sqrt{i+1}}$ as $\mathsf{SNR} \to \infty$. Hence, as $\mathsf{SNR} \to \infty$, we conclude that

$$p_1(\mathsf{SNR}) = \mathsf{SNR}^{-\frac{1}{2}}\Theta(1),$$

which implies $p_1(\mathsf{SNR}) \overset{\mathrm{e}}{=} \mathsf{SNR}^{-\frac{1}{2}}$ for $n = 2$.

We now consider the proof for $n \geq 3$ case. To that end, by using the Taylor series expansion for $\tan^{-1}(\cdot)$ [50], we can express $\rho_{\mathsf{SNR}}(\beta)$ in the high SNR regime as

$$\rho_{\mathsf{SNR}}(\beta) = \frac{\tan\left(\frac{\pi}{4}+\frac{\pi}{2^n}\right) - \tan\left(\frac{\pi}{4}-\frac{\pi}{2^n}\right)}{2(i+1)\sin^2\beta + \mathsf{SNR}},$$

by considering the first term of the series which has the smallest decay rate in terms of SNR. Hence, we can simplify $p_1(\mathsf{SNR})$ to

$$p_1(\mathsf{SNR}) = \frac{1}{2}\left\{\tan\left(\frac{\pi}{4}+\frac{\pi}{2^n}\right) - \tan\left(\frac{\pi}{4}-\frac{\pi}{2^n}\right)\right\} \int_0^{\frac{\pi}{2}} \frac{\prod_{i=0}^{N-2}\left\{2(i+1)\sin^2\beta\right\}}{\prod_{i=0}^{N-1}\left\{2(i+1)\sin^2\beta + \mathsf{SNR}\right\}} d\beta.$$

Hence, the above expression becomes

$$p_1(\mathsf{SNR}) = \frac{1}{2}\left\{\tan\left(\frac{\pi}{4}+\frac{\pi}{2^n}\right) - \tan\left(\frac{\pi}{4}-\frac{\pi}{2^n}\right)\right\}\mathsf{SNR}^{-N} \int_0^{\frac{\pi}{2}} \prod_{i=0}^{N-2}\left\{2(i+1)\sin^2\beta\right\} d\beta,$$

as $\mathsf{SNR} \to \infty$. Since $\int_0^{\frac{\pi}{2}} \prod_{i=0}^{N-2}\left\{2(i+1)\sin^2\beta\right\} d\beta \leq \infty$, we conclude that

$$p_1(\mathsf{SNR}) = \mathsf{SNR}^{-N}\Theta(1),$$

as $\mathsf{SNR} \to \infty$. This implies that $p_1(\mathsf{SNR}) \overset{\mathrm{e}}{=} \mathsf{SNR}^{-N}$ for $n \geq 3$.

The proof for $p_2(\mathsf{SNR})$ and $p_3(\mathsf{SNR})$ are similar, and we get

$$p_2(\mathsf{SNR}) \overset{\mathrm{e}}{=} \begin{cases} \mathsf{SNR}^{-\frac{1}{2}} & n = 2 \\ \mathsf{SNR}^{-N} & n \geq 3, \end{cases}$$

and

$$p_3(\mathsf{SNR}) \overset{\mathrm{e}}{=} \mathsf{SNR}^{-N},$$

for $n \geq 2$. Here, we omit the proof to avoid repetition.

Since $p(\mathsf{SNR}) = \frac{2^n N}{\pi}\left(p_1(\mathsf{SNR}) + p_2(\mathsf{SNR}) - p_3(\mathsf{SNR})\right)$, we conclude that $p(\mathsf{SNR}) \overset{\mathrm{e}}{=} \mathsf{SNR}^{-\frac{1}{2}}$ for $n = 2$ and $p(\mathsf{SNR}) \overset{\mathrm{e}}{=} \mathsf{SNR}^{-N}$ for $n \geq 3$.

Appendix D
Proof of Lemma 2

To find $p(\mathsf{SNR})$, we average (18) over the distributions of $R^\star = |H_{L^\star}|$ and $\Theta_{L^\star}$. We first find the distribution of $\Theta_{L^\star}$ and for that we take some insights from the proof of Theorem 3 of [8]. As such, without loss of generality let us assume that $x_0 = \mathrm{e}^{j\frac{\pi}{4}}$ is transmitted and $\Theta_l \in \left[-\frac{\pi}{2^n}, \frac{\pi}{2^n}\right]$ for all $l \in [0 : N-1]$. By defining $\Omega_l = |\Theta_l|$, we can write the cdf of it as $F_{\Omega_l}(\omega) = \frac{2^n}{\pi}\omega$. According to the selection rule, the detector selects $\Omega^\star$ in such a way that $\Omega^\star = \min_{l\in[0:N-1]} \Omega_l$. Thus the cdf of $\Omega^\star$ can be derived as

$$F_{\Omega^\star}(\omega^\star) = \mathsf{Pr}\left\{\Omega^\star \leq \omega^\star\right\} = 1 - \left(1 - \frac{2^n\omega^\star}{\pi}\right)^N.$$

Therefore, in the selected antenna $L^\star$ we have $\Theta_{L^\star} = \mathsf{sgn}(\Theta_{L^\star})\,\Omega^\star$ where $\mathsf{sgn}(\cdot)$ is signum function. Therefore, we can write the pdf of $\Theta_{L^\star}$ as

$$f_{\Theta_{L^\star}}(\lambda) = \frac{2^{n-1}N}{\pi}\left(1 + \frac{2^n|\lambda|}{\pi}\right)^{N-1},$$

where $|\lambda|$ is the modulus of λ.

Then the angle of the rotated constellation point $(H^\star x_0)$ will be $\Theta^\star = \Theta_{l^\star} + \frac{\pi}{4}$. Therefore, the pdf of the angle of the rotated constellation point $\Theta^\star$ can be given as

$$f_{\Theta^\star}(\theta^\star) = \begin{cases} \frac{2^{n-1}N}{\pi}\left(1 + 2^{n-2} - \frac{2^n\theta^\star}{\pi}\right)^{N-1} & \text{if} \quad \theta^\star \geq \frac{\pi}{4} \\ \frac{2^{n-1}N}{\pi}\left(1 - 2^{n-2} + \frac{2^n\theta^\star}{\pi}\right)^{N-1} & \text{if} \quad \theta^\star < \frac{\pi}{4}. \end{cases}$$

Since the pdf of Rayleigh fading magnitude in the selected antenna $L^\star$ is $f_{R^\star}(r^\star) = 2r^\star\exp\left\{-(r^\star)^2\right\}$, we can use $f_{R^\star}(r^\star)$ and $f_{\Theta^\star}(\theta^\star)$ to average $p(\mathsf{SNR}, h^\star)$ to get the SEP expression in (21).

This article has been accepted for publication in a future issue of this journal, but has not been fully edited. Content may change prior to final publication. Citation information: DOI 10.1109/OJCOMS.2021.3133526, IEEE Open Journal of the Communications Society

$$\rho_{\mathsf{SNR}}(\beta)=\int_{\frac{\pi}{4}-\frac{\pi}{2^n}}^{\frac{\pi}{4}+\frac{\pi}{2^n}}\frac{1}{\left\{(i+1)\sin^2\beta+\mathsf{SNR}\cos^2\theta\right\}}d\theta=\frac{\tan^{-1}\left[\frac{\sqrt{(i+1)\sin^2\beta\{(i+1)\sin^2\beta+\mathsf{SNR}\}}\left\{\tan\left(\frac{\pi}{4}+\frac{\pi}{2^n}\right)-\tan\left(\frac{\pi}{4}-\frac{\pi}{2^n}\right)\right\}}{2(i+1)\sin^2\beta+\mathsf{SNR}}\right]}{\sqrt{(i+1)\sin^2\beta\left\{(i+1)\sin^2\beta+\mathsf{SNR}\right\}}}. \tag{31}$$

Appendix E
Proof of Theorem 3

The $N=1$ case follows from [8]. Hence, we only focus on $N\geq 2$ case for the proof. We first define

$$p_1(\mathsf{SNR})=\int_{\frac{\pi}{4}}^{\frac{\pi}{4}+\frac{\pi}{2^n}}\int_0^{\infty}\mathcal{Q}\left(\sqrt{2\mathsf{SNR}}r\cos\theta\right)r\exp\left(-r^2\right)\left(1+2^{n-2}-\frac{2^n\theta}{\pi}\right)^{N-1}dr\,d\theta,$$

$$p_2(\mathsf{SNR})=\int_{\frac{\pi}{4}}^{\frac{\pi}{4}+\frac{\pi}{2^n}}\int_0^{\infty}\mathcal{Q}\left(\sqrt{2\mathsf{SNR}}r\sin\theta\right)r\exp\left(-r^2\right)\left(1+2^{n-2}-\frac{2^n\theta}{\pi}\right)^{N-1}dr\,d\theta,$$

$$p_3(\mathsf{SNR})=\int_{\frac{\pi}{4}}^{\frac{\pi}{4}+\frac{\pi}{2^n}}\int_0^{\infty}\mathcal{Q}\left(\sqrt{2\mathsf{SNR}}r\cos\theta\right)\mathcal{Q}\left(\sqrt{2\mathsf{SNR}}r\sin\theta\right)r\exp\left(-r^2\right)\left(1+2^{n-2}-\frac{2^n\theta}{\pi}\right)^{N-1}dr\,d\theta.$$

By using Craig's formula for $\mathcal{Q}(\cdot)$ and

$$\left(1+2^{n-2}-\frac{2^n\theta}{\pi}\right)^{N-1}=\left(1+2^{n-2}\right)^{N-1}\sum_{i=0}^{N-1}\binom{N-1}{i}\left(-\frac{2^n\theta}{\pi\left(1+2^{n-2}\right)}\right)^i$$

from the Binomial expansion, we can re-express $p_1(\mathsf{SNR})$ as

$$\begin{aligned}p_1(\mathsf{SNR})&=\left(1+2^{n-2}\right)^{N-1}\int_0^{\frac{\pi}{2}}\int_{\frac{\pi}{4}}^{\frac{\pi}{4}+\frac{\pi}{2^n}}\int_0^{\infty}\sum_{i=0}^{N-1}\binom{N-1}{i}\left(-\frac{2^n\theta}{\pi\left(1+2^{n-2}\right)}\right)^i\\&\qquad r\exp\left\{-\left(\frac{\mathsf{SNR}\cos^2\theta}{\sin^2}+1\right)r^2\right\}dr\,d\theta\,d\beta\\&=\frac{\left(1+2^{n-2}\right)^{N-1}}{2}\int_0^{\frac{\pi}{2}}\sin^2\beta\int_{\frac{\pi}{4}}^{\frac{\pi}{4}+\frac{\pi}{2^n}}\sum_{i=0}^{N-1}\binom{N-1}{i}\left(-\frac{2^n}{\pi\left(1+2^{n-2}\right)}\right)^i\\&\qquad\frac{\theta^i}{\mathsf{SNR}\cos^2\theta+\sin^2\beta}d\theta\,d\beta.\end{aligned}$$

Let

$$g_{\mathsf{SNR}}(\theta,\beta)=\frac{\left(1+2^{n-2}\right)^{N-1}}{2}\sin^2\beta\sum_{i=0}^{N-1}\binom{N-1}{i}\left(-\frac{2^n}{\pi\left(1+2^{n-2}\right)}\right)^i\frac{\theta^i}{\mathsf{SNR}\cos^2\theta+\sin^2\beta}$$

be a collection of functions indexed by SNR. The function $g_{\mathsf{SNR}}(\theta,\beta)$ becomes

$$g_{\infty}(\theta,\beta)=\mathsf{SNR}^{-1}\frac{\left(1+2^{n-2}\right)^{N-1}}{2}\sin^2\beta\sum_{i=0}^{N-1}\binom{N-1}{i}\left(-\frac{2^n}{\pi\left(1+2^{n-2}\right)}\right)^i\frac{\theta^i}{\cos^2\theta}$$

as $\mathsf{SNR}\to\infty$. Further, by using [50, eq. 2.643(9)], we get $\int_0^{\frac{\pi}{2}}\int_{\frac{\pi}{4}}^{\frac{\pi}{4}+\frac{\pi}{2^n}}g_{\infty}(\theta,\beta)\,d\theta d\beta<\infty$ for $N\geq 2$. Hence, as $\mathsf{SNR}\to\infty$, we conclude that

$$p_1(\mathsf{SNR})=\mathsf{SNR}^{-1}\Theta(1)$$

by using the monotone convergence theorem [51]. Therefore, $p_1(\mathsf{SNR})\overset{\mathrm{e}}{=}\mathsf{SNR}^{-1}$.

The proof for $p_2(\mathsf{SNR})$ and $p_3(\mathsf{SNR})$ follow similar steps and we get $p_2(\mathsf{SNR})\overset{\mathrm{e}}{=}\mathsf{SNR}^{-1}$ and $p_3(\mathsf{SNR})\overset{\mathrm{e}}{=}\mathsf{SNR}^{-1}$. Here, we omit the proof to avoid repetition.

Since $p(\mathsf{SNR})=\frac{2^{n+1}N}{\pi}\left(p_1(\mathsf{SNR})+p_2(\mathsf{SNR})-p_3(\mathsf{SNR})\right)$, we conclude that $p(\mathsf{SNR})\overset{\mathrm{e}}{=}\mathsf{SNR}^{-1}$ for $n\geq 2$ and $N\geq 2$.

We also note that for $N=1$ case, the system becomes SISO and by following similar steps as given in the proof of Theorem 4 of [8], we get $\mathsf{DVO}=\frac{1}{2}$ for $n=2$ and $\mathsf{DVO}=1$ for $n\geq 3$.

Appendix F
Proof of Lemma 3

To prove Lemma 3, we first obtain the following result.

Lemma 4: Consider a finite sequence of random variables

$$(U_0,V_0),(U_1,V_1)\cdots(U_{N-1},V_{N-1}),$$

where $U_0,\cdots U_{N-1},V_0,\cdots V_{N-1}$ are all iid with a common pdf of $f(u)$ and cdf of $F(u)$. The joint pdf of U_l and V_l is given as

$$f_{U_l,V_l}(u,v)=\begin{cases}\frac{f(u)f(v)}{P_{\alpha}} & \text{if } (u,v)\in\mathcal{S}_{\alpha}\\ 0 & \text{otherwise,}\end{cases}$$

where $\mathcal{S}_{\alpha}$ is the convex cone given as

$$\mathcal{S}_{\alpha}=\left\{(u,v)\in\mathbb{R}^2:\frac{\pi}{4}-\alpha\leq\tan^{-1}\left(\frac{v}{u}\right)\leq\frac{\pi}{4}+\alpha\right\},$$

This article has been accepted for publication in a future issue of this journal, but has not been fully edited. Content may change prior to final publication. Citation information: DOI 10.1109/OJCOMS.2021.3133526, IEEE Open Journal of the Communications Society

and P_α is the normalization coefficient given as

$$\begin{aligned} P_\alpha &= \int_0^\infty \int_{u\tan\left(\frac{\pi}{4}-\alpha\right)}^{u\tan\left(\frac{\pi}{4}+\alpha\right)} f(v) f(u)\, dv\, du, \\ &= \int_0^\infty f(u) F\left(u\tan\left(\frac{\pi}{4}+\alpha\right)\right) \\ &\qquad - f(u) F\left(u\tan\left(\frac{\pi}{4}-\alpha\right)\right) du. \end{aligned}$$

Let $Z_l^{\mathsf{min}} = \min\{U_l, V_l\}$, $Z_l^{\mathsf{max}} = \max\{U_l, V_l\}$, $Z_{L^\star}^{\mathsf{min}} = \max_{l\in[0:N-1]} Z_l^{\mathsf{min}}$, and $L^\star = \arg\max_{l\in[0:N-1]} Z_l^{\mathsf{min}}$. Further, let E_l be the event such that $E_l \triangleq \left\{Z_{L^\star}^{\mathsf{min}} = Z_l^{\mathsf{min}}\right\}$, and $g_{Z_{L^\star}^{\mathsf{min}}}(z)$ be the the pdf of $Z_{L^\star}^{\mathsf{min}}$. Then, $f_{Z_{L^\star}^{\mathsf{min}}, Z_{L^\star}^{\mathsf{max}}}(u,v) = f_{Z_0^{\mathsf{min}}, Z_0^{\mathsf{max}}|E_0}(u,v)$, and $f_{Z_{L^\star}^{\mathsf{min}}, Z_{L^\star}^{\mathsf{max}}}(u,v)$ is given by

$$f_{Z_{L^\star}^{\mathsf{min}}, Z_{L^\star}^{\mathsf{max}}}(u,v) = \begin{cases} \frac{f(v) g_{Z_{L^\star}^{\mathsf{min}}}(u)}{F\left(u\tan\left(\frac{\pi}{4}+\alpha\right)\right) - F(u)} & \text{if } v \geq u \\ 0 & \text{otherwise.} \end{cases} \tag{32}$$

Proof: To start the proof, We can write

$$f_{Z_{L^\star}^{\mathsf{min}}, Z_{L^\star}^{\mathsf{max}}}(u,v) = \sum_{l=0}^{N-1} \mathsf{Pr}\{E_l\} f_{Z_l^{\mathsf{min}}, Z_l^{\mathsf{max}}|E_l}(u,v).$$

Since $\mathsf{Pr}\{E_l\} = \frac{1}{N}$ and $f_{Z_l^{\mathsf{min}}, Z_l^{\mathsf{max}}|E_l}(u,v) = f_{Z_0^{\mathsf{min}}, Z_0^{\mathsf{max}}|E_l}(u,v)$ for all $l \in [0:N-1]$, we have $f_{Z_{L^\star}^{\mathsf{min}}, Z_{L^\star}^{\mathsf{max}}}(u,v) = f_{Z_0^{\mathsf{min}}, Z_0^{\mathsf{max}}|E_0}(u,v)$. To that end, we then find $F_{Z_0^{\mathsf{min}}, Z_0^{\mathsf{max}}|E_0}(u,v)$ which is the joint cdf of Z_0^{min} and Z_0^{max} conditioned on the event E_0. By defining $Z_{-0}^\star = \max_{l\in[1:N-1]} Z_l^{\mathsf{min}}$, we can represent the event E_0 as $E_0 \triangleq \left\{Z_0^{\mathsf{min}} \geq Z_{-0}^\star\right\}$. Let us further define $g_{Z_{-0}^\star}(z)$ and $G_{Z_{-0}^\star}(z)$ to be the pdf and cdf of $Z_{-0}^\star$, respectively.

Then, for $v \geq u$, we have $F_{Z_0^{\mathsf{min}}, Z_0^{\mathsf{max}}|E_0}(u,v) = \mathsf{Pr}\left\{Z_0^{\mathsf{min}} \leq u, Z_0^{\mathsf{max}} \leq v \,|\, Z_0^{\mathsf{min}} \geq Z_{-0}^\star\right\}$. By using the Bayes' theorem, we can write $F_{Z_0^{\mathsf{min}}, Z_0^{\mathsf{max}}|E_0}(u,v) = N\mathsf{Pr}\left\{Z_{-0}^\star \leq Z_0^{\mathsf{min}} \leq u, Z_0^{\mathsf{max}} \leq v\right\}$. Further, by conditioning on the event $Z_{-0}^\star = z$, we can write

$$\begin{aligned} &F_{Z_0^{\mathsf{min}}, Z_0^{\mathsf{max}}|E_0}(u,v) = \\ &\quad N\int_0^u \mathsf{Pr}\left\{z \leq Z_0^{\mathsf{min}} \leq u, Z_0^{\mathsf{max}} \leq v \,|\, Z_{-0}^\star = z\right\} \\ &\qquad g_{Z_{-0}^\star}(z)\, dz. \end{aligned}$$

Due to the independence of $Z_{-0}^\star$ from (U_0, V_0), we can re-write the above expression as

$$\begin{aligned} &F_{Z_0^{\mathsf{min}}, Z_0^{\mathsf{max}}|E_0}(u,v) = \\ &\quad N\int_0^u \mathsf{Pr}\left\{z \leq Z_0^{\mathsf{min}} \leq u, Z_0^{\mathsf{max}} \leq v\right\} g_{Z_{-0}^\star}(z)\, dz. \end{aligned}$$

Considering the symmetry of the problem, we note that

$$\begin{aligned} &\mathsf{Pr}\left\{z \leq Z_0^{\mathsf{min}} \leq u, Z_0^{\mathsf{max}} \leq v\right\} = \\ &\qquad 2\,\mathsf{Pr}\left\{z \leq U_0 \leq u, U_0 \leq V_0 \leq v\right\}. \end{aligned}$$

Therefore, we have

$$\begin{aligned} &F_{Z_0^{\mathsf{min}}, Z_0^{\mathsf{max}}|E_0}(u,v) = \\ &\quad 2N\int_0^u \mathsf{Pr}\left\{z \leq U_0 \leq u, U_0 \leq V_0 \leq v\right\} g_{Z_{-0}^\star}(z)\, dz. \end{aligned}$$

Using the above expression, we can write the joint pdf of Z_0^{min} and Z_0^{max} given the event E_0 as

$$\begin{aligned} &f_{Z_0^{\mathsf{min}}, Z_0^{\mathsf{max}}|E_0}(u,v) \\ &\quad = \begin{cases} \frac{2N}{P_\alpha} f(v) f(u) G_{Z_{-0}^\star}(u) & \text{if } (u,v) \in \mathcal{S}_\alpha \\ 0 & \text{otherwise,} \end{cases} \end{aligned} \tag{33}$$

where $G_{Z_{-0}^\star}(u) = \mathsf{Pr}\left\{Z_{-0}^\star \leq u\right\}$ and $v \geq u$. Since $g_{Z_{L^\star}^{\mathsf{min}}}(u) = \frac{\partial}{\partial u}\mathsf{Pr}\left\{Z_0^{\mathsf{min}} \leq u\right\}^N$, we can write $g_{Z_{L^\star}^{\mathsf{min}}}(u) = N G_{Z_{-0}^\star}(u) f_{Z_0^{\mathsf{min}}}(u)$.

We then focus on finding $f_{Z_0^{\mathsf{min}}}(u)$. To that end, we first find the cdf $F_{Z_0^{\mathsf{min}}}(u)$ where

$$\begin{aligned} F_{Z_0^{\mathsf{min}}}(u) &= \mathsf{Pr}\left\{Z_0^{\mathsf{min}} \leq u\right\} \\ &= 2\,\mathsf{Pr}\left\{U_0 \leq u, V_0 \geq U_0\right\} \\ &= 2\int_0^u \mathsf{Pr}\left\{V_0 \geq t \,|\, U_0 = t\right\} f(t)\, dt \\ &= \frac{2}{P_\alpha}\int_0^u \left[F\left(t\tan\left(\frac{\pi}{4}+\alpha\right)\right) - F(t)\right] f(t)\, dt. \end{aligned}$$

Therefore, we have

$$f_{Z_0^{\mathsf{min}}}(u) = \frac{2}{P_\alpha} f(u)\left[F\left(u\tan\left(\frac{\pi}{4}+\alpha\right)\right) - F(u)\right].$$

Using the above expression, we now can write

$$\begin{aligned} g_{Z_{L^\star}^{\mathsf{min}}}(u) = &\frac{2N}{P_\alpha} G_{Z_{-0}^\star}(u) \\ &f(u)\left[F\left(u\tan\left(\frac{\pi}{4}+\alpha\right)\right) - F(u)\right]. \end{aligned} \tag{34}$$

By substituting $G_{Z_{-0}^\star}(u)$ using the expression (34) in (33), we get the expression (32). That concludes the proof. ■

We now use Lemma 4 to prove Lemma 3. To this end, we will only focus on the event where H_l is in $\mathcal{D}_{2^{n-1}}$ for all $l \in [0:N-1]$ without loss of generality. Calculating the conditional SEP on this event will give the unconditioned SEP due to spherical symmetry in the fading process. On this event, the distances to the decision boundaries are given by the absolute values of real and imaginary parts of $\sqrt{\mathsf{SNR}} H_l e^{\jmath\frac{\pi}{4}}$ for all transmitted symbols $X \in \mathcal{C}$. Using this observation, we define $U_l \triangleq \left|\mathsf{Re}\left(\sqrt{\mathsf{SNR}} H_l e^{\jmath\frac{\pi}{4}}\right)\right|$ and $V_l \triangleq \left|\mathsf{Im}\left(\sqrt{\mathsf{SNR}} H_l e^{\jmath\frac{\pi}{4}}\right)\right|$. We use Fig. 14 as a visual guide to illustrate this situation, where $(U_l, V_l) \in \mathcal{S}_{\frac{\pi}{2^n}}$ on this event. Further, under Rayleigh fading, we have $f(u) = \frac{2}{\sqrt{\pi\mathsf{SNR}}}\exp\left(-\frac{u^2}{\mathsf{SNR}}\right)$, $F(u) = 1 - 2\mathcal{Q}\left(\frac{\sqrt{2}u}{\sqrt{\mathsf{SNR}}}\right)$ and $P_{\frac{\pi}{2^n}} = \frac{1}{2^{n-2}}$.

By following steps which are similar to obtain (18), we can write

$$\begin{aligned} p(\mathsf{SNR}, h^\star) = &\mathcal{Q}\left(\sqrt{2}u\right) + \mathcal{Q}\left(\sqrt{2}v\right) - \\ &\mathcal{Q}\left(\sqrt{2}u\right)\mathcal{Q}\left(\sqrt{2}v\right), \end{aligned} \tag{35}$$

This article has been accepted for publication in a future issue of this journal, but has not been fully edited. Content may change prior to final publication. Citation information: DOI 10.1109/OJCOMS.2021.3133526, IEEE Open Journal of the Communications Society

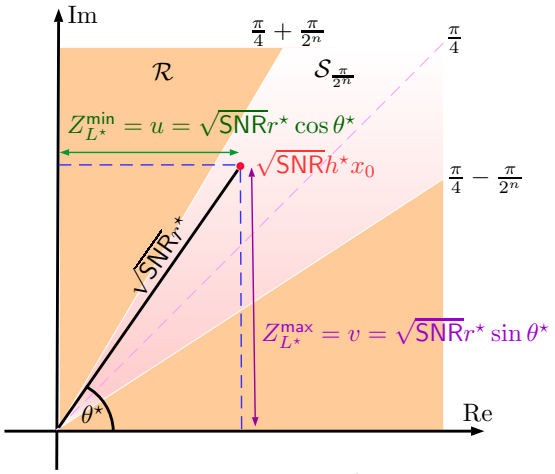

Figure 14: An illustration of the average SEP calculation under the max-distance antenna selection strategy. Without loss of generality, let us assume that the x_0 is transmitted and the region of attraction is $\mathcal{R}=\left\{z\in\mathbb{C}:0\leq \mathsf{Arg}\left(z\right)\leq\frac{\pi}{2}\right\}$. Then, the distances to the decision boundaries are $Z_{L^\star}^{\min}=u$ and $Z_{L^\star}^{\max}=v$. Using polar coordinates, we can represent these distances as $Z_{L^\star}^{\min}=\sqrt{\mathsf{SNR}}r^\star\cos\theta^\star$ and $Z_{L^\star}^{\max}=\sqrt{\mathsf{SNR}}r^\star\sin\theta^\star$ where $r^\star=|h^\star|$ and $\theta^\star=\mathsf{Arg}\left(h^\star x_0\right)$.

given that $Z_{L^\star}^{\min}=u$ and $Z_{L^\star}^{\max}=v$. We then can obtain $p\left(\mathsf{SNR}\right)$ by averaging the above expression with respect to the joint pdf of $Z_{L^\star}^{\min}$ and $Z_{L^\star}^{\max}$, which can be given as

$$f_{Z_{L^\star}^{\min},Z_{L^\star}^{\max}}\left(u,v\right)=\begin{cases}\frac{2^{n+1}N}{\pi\mathsf{SNR}}G_{Z_{-0}^\star}\left(u\right)\exp\left(-\frac{u^2+v^2}{\mathsf{SNR}}\right) & \text{if } (u,v)\in\mathcal{S}_{\frac{\pi}{2^n}}\\ 0 & \text{otherwise,}\end{cases}\tag{36}$$

where $G_{Z_{-0}^\star}\left(u\right)=\left\{F_{Z_0^{\min}}\left(u\right)\right\}^{N-1}$ with

$$\begin{aligned}F_{Z_0^{\min}}\left(u\right)&=\frac{2}{P_{\frac{\pi}{2^n}}}\int_0^u\left\{F\left(t\tan\left(\frac{\pi}{4}+\frac{\pi}{2^n}\right)-F\left(t\right)\right)\right\}f\left(t\right)\,dt\\&=\frac{2}{P_{\frac{\pi}{2^n}}}\int_0^u F\left(t\tan\left(\frac{\pi}{4}+\frac{\pi}{2^n}\right)\right)f\left(t\right)\,dt-\frac{F^2\left(u\right)}{P_{\frac{\pi}{2^n}}},\end{aligned}$$

being the cdf of $Z_0^{\min}$. By substituting the corresponding functions, we get the expression (37) for general n-bit quantization. For $n=2$ case, we can further simplify the above expression to

$$F_{Z_0^{\min}}\left(u\right)=1-4\mathcal{Q}^2\left(\frac{\sqrt{2}u}{\sqrt{\mathsf{SNR}}}\right).$$

Therefore for $(u,v)\in\mathcal{S}_{\frac{\pi}{2^n}}$, we can write

$$f_{Z_{L^\star}^{\min},Z_{L^\star}^{\max}}\left(u,v\right)=\frac{2^{n+1}N}{\pi\mathsf{SNR}}\left\{F_{Z_0^{\min}}\left(u\right)\right\}^{N-1}\exp\left(-\frac{u^2+v^2}{\mathsf{SNR}}\right).\tag{38}$$

By averaging the expression (35) over the above joint distribution $f_{Z_{L^\star}^{\min},Z_{L^\star}^{\max}}\left(u,v\right)$, we get the $p\left(\mathsf{SNR}\right)$. By using the change of variables $u=\sqrt{\mathsf{SNR}}r^\star\cos\theta^\star$ and $v=\sqrt{\mathsf{SNR}}r^\star\sin\theta^\star$, we can convert the $p\left(\mathsf{SNR}\right)$ expression to the format given in Lemma 3.

Appendix G
Proof of Theorem 4

The proof for the $n=2$ and $N=1$ case follows directly from [8]. To obtain the proof for $n\geq 3$, we first observe that the symbol error probability expression given in (23) is smaller than the one in (19). This is due to the construction of the max-distance antenna selection strategy, which selects the antenna that is furthest away from the decision boundaries. Hence, the DVO achieved by the max-norm antenna selection strategy forms a lower bound for the DVO achieved by the max-distance antenna selection strategy. Since the DVO for the max-norm strategy is equal to the high-resolution quantization upper bound N for $n\geq 3$, we conclude that the max-distance DVO is also equal to N for $n\geq 3$.

The final remaining case to prove is the one where $N=2$ and $n=2$, which we will prove by using Lemma 3. We start the proof for this case by defining

$$\begin{aligned}p_1\left(\mathsf{SNR}\right)&=\int_{\frac{\pi}{4}}^{\frac{\pi}{2}}\int_0^\infty\mathcal{Q}\left(\sqrt{2\mathsf{SNR}}r\cos\theta\right)\\&\qquad\left[1-4\mathcal{Q}^2\left(\sqrt{2}r\cos\theta\right)\right]^{N-1}r\exp\left(-r^2\right)dr\,d\theta,\\p_2\left(\mathsf{SNR}\right)&=\int_{\frac{\pi}{4}}^{\frac{\pi}{2}}\int_0^\infty\mathcal{Q}\left(\sqrt{2\mathsf{SNR}}r\sin\theta\right)\\&\qquad\left[1-4\mathcal{Q}^2\left(\sqrt{2}r\cos\theta\right)\right]^{N-1}r\exp\left(-r^2\right)dr\,d\theta,\\p_3\left(\mathsf{SNR}\right)&=\int_{\frac{\pi}{4}}^{\frac{\pi}{2}}\int_0^\infty\mathcal{Q}\left(\sqrt{2\mathsf{SNR}}r\cos\theta\right)\\&\qquad\mathcal{Q}\left(\sqrt{2\mathsf{SNR}}r\sin\theta\right)\left[1-4\mathcal{Q}^2\left(\sqrt{2}r\cos\theta\right)\right]^{N-1}\\&\qquad r\exp\left(-r^2\right)dr\,d\theta,\end{aligned}$$

where $\mathcal{Q}\left(x\right)=\frac{1}{\pi}\int_0^{\frac{\pi}{2}}\exp\left(-\frac{x^2}{2\sin^2\beta}\right)d\beta$ and $\mathcal{Q}^2\left(x\right)=\frac{1}{\pi}\int_0^{\frac{\pi}{4}}\exp\left(-\frac{x^2}{2\sin^2\beta}\right)d\beta$ [52]. We further can express $\left[1-4\mathcal{Q}^2\left(\sqrt{2}r\cos\theta\right)\right]^{N-1}=\sum_{i=0}^{N-1}\binom{N-1}{i}\left(-4\right)^i\mathcal{Q}^{2i}\left(\sqrt{2}r\cos\theta\right)$ using the Binomial expansion, and hence we can re-express $p_1\left(\mathsf{SNR}\right)$ as

$$\begin{aligned}p_1\left(\mathsf{SNR}\right)=\int_0^{\frac{\pi}{4}}\cdots\int_0^{\frac{\pi}{4}}\int_0^{\frac{\pi}{2}}\int_{\frac{\pi}{4}}^{\frac{\pi}{2}}\int_0^\infty\sum_{i=0}^{N-1}\binom{N-1}{i}\frac{\left(-4\right)^i}{\pi^{i+1}}\\r\exp\left\{-r^2\left(1+\frac{\mathsf{SNR}\cos^2\theta}{\sin^2\beta}+\sum_{p=1}^{i}\frac{\mathsf{sgn}\left(i\right)\cos^2\theta}{\sin^2\gamma_p}\right)\right\}\\dr\,d\theta\,d\beta\,d\gamma_1\cdots d\gamma_i,\end{aligned}$$

where $\mathsf{sgn}\left(\cdot\right)$ is given as

$$\mathsf{sgn}\left(a\right)=\begin{cases}1 & \text{if } a\geq 0\\-1 & \text{if } a<0.\end{cases}$$

This article has been accepted for publication in a future issue of this journal, but has not been fully edited. Content may change prior to final publication. Citation information: DOI 10.1109/OJCOMS.2021.3133526, IEEE Open Journal of the Communications Society

$$F_{Z_0^{\min}}(u) = \frac{2^n}{\sqrt{\pi \mathsf{SNR}}} \int_0^u \left\{ 1 - 2\mathcal{Q}\left(\frac{\sqrt{2}t}{\sqrt{\mathsf{SNR}}} \tan\left(\frac{\pi}{4} + \frac{\pi}{2^n} \right) \right) \right\} \exp\left(-\frac{t^2}{\mathsf{SNR}} \right) dt - 2^{n-2} \left\{ 1 - 2\mathcal{Q}\left(\frac{\sqrt{2}u}{\sqrt{\mathsf{SNR}}} \right) \right\}^2 \quad (37)$$

Using [50], we can simplify the above expression as

$$\begin{aligned} p_1(\mathsf{SNR}) &= \int_0^{\frac{\pi}{4}} \cdots \int_0^{\frac{\pi}{4}} \int_0^{\frac{\pi}{2}} \int_{\frac{\pi}{4}}^{\frac{\pi}{2}} \sum_{i=0}^{N-1} \binom{N-1}{i} \frac{(-4)^i}{\pi^{i+1}} \\ &\qquad \frac{1}{2\left(1 + B\cos^2\theta\right)} d\theta\, d\beta\, d\gamma_1 \cdots d\gamma_i, \\ &= \int_0^{\frac{\pi}{4}} \cdots \int_0^{\frac{\pi}{4}} \int_0^{\frac{\pi}{2}} \sum_{i=0}^{N-1} \binom{N-1}{i} \frac{(-4)^i}{\pi^{i+1}} \\ &\qquad \frac{\tan^{-1}(1+B)}{2\sqrt{1+B}}\, d\beta\, d\gamma_1 \cdots d\gamma_i, \end{aligned}$$

where $B = \frac{\mathsf{SNR}}{\sin^2\beta} + \sum_{p=1}^{i} \frac{\mathsf{sgn}(i)}{\sin^2\gamma_p}$. Using the Taylor series expansion [50], in the high SNR regime $\tan^{-1}(1+B)$ converges to $\frac{\pi}{2}$. Therefore,

$$\begin{aligned} p_1(\mathsf{SNR}) &= \int_0^{\frac{\pi}{4}} \cdots \int_0^{\frac{\pi}{4}} \int_0^{\frac{\pi}{2}} \sum_{i=0}^{N-1} \binom{N-1}{i} \frac{(-4)^i}{4\pi^i} \\ &\qquad \frac{1}{\sqrt{1+B}}\, d\beta\, d\gamma_1 \cdots d\gamma_i, \end{aligned}$$

as $\mathsf{SNR} \to \infty$.

By substituting $N = 2$ in the above expression we get

$$\begin{aligned} p_1(\mathsf{SNR}) &= \frac{1}{4} \int_0^{\frac{\pi}{2}} \frac{1}{\sqrt{1 + \frac{\mathsf{SNR}}{\sin^2\beta}}}\, d\beta \\ &\quad - \frac{1}{\pi} \int_0^{\frac{\pi}{4}} \int_0^{\frac{\pi}{2}} \frac{1}{\sqrt{1 + \frac{\mathsf{SNR}}{\sin^2\beta} + \frac{1}{\sin^2\gamma_1}}}\, d\beta\, d\gamma_1. \end{aligned}$$

By doing further mathematical manipulations, we get

$$p_1(\mathsf{SNR}) = \frac{16}{\pi^2} \int_0^{\frac{\pi}{2}} \frac{1}{1 + \frac{\mathsf{SNR}}{\sin^2\beta}} d\beta, \quad (39)$$

as $\mathsf{SNR} \to \infty$. Therefore, we conclude that $p_1(\mathsf{SNR}) \stackrel{\mathrm{e}}{=} \mathsf{SNR}^{-1}$ as $\mathsf{SNR} \to \infty$.

The proof for $p_2(\mathsf{SNR})$ and $p_3(\mathsf{SNR})$ follow similar steps and we get $p_2(\mathsf{SNR}) \stackrel{\mathrm{e}}{=} \mathsf{SNR}^{-1}$ and $p_3(\mathsf{SNR}) \stackrel{\mathrm{e}}{=} \mathsf{SNR}^{-1}$. Here, we omit the proof to avoid repetition. Therefore, we can conclude that $p(\mathsf{SNR}) \stackrel{\mathrm{e}}{=} \mathsf{SNR}^{-1}$ for $n = 2$ and $N = 2$. Hence, the DVO is equal to $\frac{N}{2}$ for this case.

REFERENCES

[1] J. Zhang, L. Dai, S. Sun, and Z. Wang, "On the spectral efficiency of massive MIMO systems with low-resolution ADCs," *IEEE Commun. Lett.*, vol. 20, no. 5, pp. 842–845, 2016.

[2] J. Zhang, L. Dai, X. Li, Y. Liu, and L. Hanzo, "On low-resolution ADCs in practical 5G millimeter-wave massive MIMO systems," *IEEE Commun. Mag.*, vol. 56, no. 7, pp. 205–211, Jul. 2018.

[3] J. Liu, Z. Luo, and X. Xiong, "Low-resolution ADCs for wireless communication: A comprehensive survey," *IEEE Access*, vol. 7, pp. 91 291–91 324, 2019.

[4] Y. Jeon, N.Lee, and V. Poor, "Robust data detection for MIMO systems with one-bit ADCs: A reinforcement learning approach," *IEEE Trans. Wireless Commun.*, vol. 19, no. 3, pp. 1663–1676, March 2020.

[5] Q. Bai and J. A. Nossek, "Energy efficiency maximization for 5G multi-antenna receivers," *Trans. Emerging Telecommunications Technologies*, vol. 26, pp. 3–14, 2015.

[6] B. Murmann, "ADC performance survey 1997-2020." [Online]. Available: http://web.stanford.edu/~murmann/adcsurvey.html

[7] S. Gayan, H. Inaltekin, R. Senanayake, and J. Evans, "Phase modulated communication with low-resolution ADCs," *Proc. IEEE International Conference on Communications (ICC)*, pp. 1–6, May 2019.

[8] S. Gayan, R. Senanayake, H. Inaltekin, and J. Evans, "Low-resolution quantization in phase modulated systems: Optimum detectors and error rate analysis," *IEEE Open Journal of the Communications Society*, vol. 1, pp. 1000–1021, 2020.

[9] N. I. Bernardo, J. Zhu, and J. Evans, "On the capacity-achieving input of channels with phase quantization," 2021. [Online]. Available: https://arxiv.org/abs/2106.11007

[10] S. Krone and G. Fettweis, "Fading channels with 1-bit output quantization: Optimal modulation, ergodic capacity and outage probability," in *2010 IEEE Information Theory Workshop*, Dublin, Ireland, Aug 2010, pp. 1–5.

[11] J. Choi, D. J. Love, D. R. Brown, and M. Boutin, "Quantized distributed reception for MIMO wireless systems using spatial multiplexing," *IEEE Trans. Signal Process.*, vol. 63, no. 13, pp. 3537–3548, Jul. 2015.

[12] S. Rangan, T. S. Rappaport, and E. Erkip, "Millimeter-wave cellular wireless networks: Potentials and challenges," *Proc. IEEE*, vol. 102, no. 3, pp. 366–385, Mar. 2014.

[13] J. H. Winters, J. Salz, and R. D. Gitlin, "The impact of antenna diversity on the capacity of wireless communication systems," *IEEE Transactions on Communications*, vol. 42, no. 234, pp. 1740–1751, 1994.

[14] A. Duel-Hallen, "Decorrelating decision-feedback multiuser detector for synchronous code-division multiple-access channel," *IEEE Trans. Commun.*, vol. 41, pp. 285–290, Feb. 1993.

[15] U. Madhow and M. Honig, "MMSE interference suppression for direct-sequence spread-spectrum CDMA," *IEEE Trans. Commun.*, vol. 42, pp. 3178–3188, Dec. 1994.

[16] H. Poor and S. Verdu, "Probability of error in MMSE multiuser detection," *IEEE Trans. Inf. Theory*, vol. 43, pp. 858–871, May 1997.

[17] E. Andersen, "Asymptotic properties of conditional maximum likelihood estimators," *Journal of the Royal Statistical Society*, vol. 32, no. 2, pp. 283–301, 1970.

[18] J. Choi, J. Mo, and R. W. Heath, "Near maximum-likelihood detector and channel estimator for uplink multiuser massive MIMO systems with one-bit ADCs," *IEEE Trans. Commun.*, vol. 64, no. 5, pp. 2005–2018, May 2016.

[19] A. Mezghani, M. S. Khoufi, and J. A. Nossek, "Maximum likelihood detection for quantized MIMO systems," in *Proc. 2008 International ITG Workshop on Smart Antennas*, Feb. 2008, pp. 278–284.

[20] Y. Jeon, N. Lee, S. Hong, and R. W. Heath, "One-bit sphere decoding for uplink massive MIMO systems with one-bit ADCs," *IEEE Trans. Wireless Commun.*, vol. 17, no. 7, pp. 4509–4521, 2018.

[21] Z. Shao, R. C. de Lamare, and L. T. N. Landau, "Iterative detection and decoding for large-scale multiple-antenna systems with 1-bit ADCs," *IEEE Trans. Wireless Commun. Lett.*, vol. 7, no. 3, pp. 476–479, 2018.

[22] Y. Jeon, H. Do, S. Hong, and N.Lee, "Soft-output detection methods for sparse millimeter-wave MIMO systems with low-precision ADCs," *IEEE Trans. Commun.*, vol. 67, no. 4, pp. 2822–2836, April 2019.

[23] A. Mezghani, M. S. Khoufi, and J. A. Nossek, "A modified MMSE receiver for quantized MIMO systems," in *Proc. Int. ITG/IEEE Workshop on Smart Antennas (WSA)*, Vienna, Austria, 2007.

[24] A. Mezghani, M. Rouatbi, and J. A. Nossek, "An iterative receiver for quantized MIMO systems," in *Proc. 2012 16th IEEE Mediterranean Electrotechnical Conference*, Yasmine Hammamet, Tunisia, Mar. 2012, pp. 1049–1052.

[25] Y. Jeon, H. Lee, and N. Lee, "Robust MLSD for wideband SIMO systems with one-bit ADCs: Reinforcement-learning approach," in *IEEE Int. Conf. Commun. Workshops (ICC Workshops)*, Kansas City, MO, USA, May 2018, pp. 1–6.

[26] S. K. J. Chae and S. Hong, "Machine learning detectors for MU-MIMO systems with one-bit ADCs," *IEEE Access*, vol. 8, pp. 86 608–86 616, May 2020.

[27] J. Mo and R. W. Heath, "Capacity analysis of one-bit quantized MIMO systems with transmitter channel state information," *IEEE Trans. Signal Process.*, vol. 63, no. 20, pp. 5498–5512, Oct. 2015.

[28] ——, "High SNR capacity of millimeter wave MIMO systems with one-bit quantization," in *Proc. 2014 Information Theory and Applications Workshop (ITA)*, San Diego, California, USA, Feb. 2014, pp. 1–5.

[29] A. Mezghani and J. A. Nossek, "Analysis of 1-bit output noncoherent fading channels in the low SNR regime," in *Proc. 2009 IEEE International Symposium on Information Theory*, Seoul, Korea, Jun. 2009, pp. 1080–1084.

[30] ——, "On ultra-wideband MIMO systems with 1-bit quantized outputs: Performance analysis and input optimization," in *Proc. 2007 IEEE International Symposium on Information Theory*, Nice, France, Jun. 2007, pp. 1286–1289.

[31] Y. Li, C. Tao, A. L. Swindlehurst, A. Mezghani, and L. Liu, "Downlink achievable rate analysis in massive MIMO systems with one-bit DACs," *IEEE Commun. Lett.*, vol. 21, no. 7, pp. 1669–1672, Jul. 2017.

[32] J. Singh and U. Madhow, "Phase-quantized block noncoherent communication," *IEEE Trans. Commun.*, vol. 61, no. 7, pp. 2828–2839, Jul. 2013.

[33] S. Gayan, R. Senanayake, H. Inaltekin, and J. Evans, "Selection combining for multi-antenna communication with low-resolution ADCs," in *2021 IEEE International Symposium on Information Theory (ISIT)*, 2021, pp. 3343–3348.

[34] R. Remmert, *Theory of Complex Functions*. New York: Springer-Verlag, 1991.

[35] B. Picinbono, "On circularity," *IEEE Trans. Signal Process.*, vol. 42, no. 12, pp. 3473–3482, Dec. 1994.

[36] E. Ollila, D. E. Tyler, V. Koivunen, and H. V. Poor, "Complex elliptically symmetric distributions: Survey, new results and applications," *IEEE Trans. Signal Process.*, vol. 60, no. 11, pp. 5597–5625, Nov. 2012.

[37] D. Tse and P. Viswanath, *Fundamentals of Wireless Communication*. New York, NY, USA: Cambridge University Press, 2005.

[38] R. G. Gallager, *Principles of Digital Communication*. New York, NY, USA: Cambridge University Press, 2008.

[39] R. W. Lucky and J. C. Hancock, "On the optimum performance of n-ary systems having two-degrees of freedom," *IRE Trans. Commun. Syst.*, vol. 10, no. 2, pp. 185–192, Jun. 1962.

[40] N. I. Bernardo, J. Zhu, and J. Evans, "Is phase shift keying optimal for channels with phase-quantized output?" in *2021 IEEE International Symposium on Information Theory (ISIT)*, 2021, pp. 634–639.

[41] P. Nazari, B. Chun, F. Tzeng, and P. Heydari, "Polar quantizer for wireless receivers: Theory, analysis, and CMOS implementation," *IEEE Trans. Circuits Syst. I, Reg. Papers*, vol. 61, no. 3, pp. 877–887, 2014.

[42] O. Dabeer and U. Madhow, "Channel estimation with low-precision analog-to-digital conversion," in *2010 IEEE International Conference on Communications*, Cape Town, South Africa, May 2010, pp. 1–6.

[43] N. Liang and W. Zhang, "Mixed-ADC massive MIMO," *IEEE J. Sel. Areas Commun.*, vol. 34, no. 4, pp. 983–997, April 2016.

[44] M. T. Ivrlac and J. A. Nossek, "On MIMO channel estimation with single-bit signal-quantization," in *Proc. Int. ITG/IEEE Workshop on Smart Antennas (WSA)*, Feb. 2007, pp. 1–7.

[45] A. Mezghani, F. Antreich, and J. A. Nossek, "Multiple parameter estimation with quantized channel output," in *Proc. 2010 International ITG Workshop on Smart Antennas (WSA)*, Feb 2010, pp. 143–150.

[46] J. Mo, P. Schniter, and R. W. Heath, "Channel estimation in broadband millimeter wave MIMO systems with few-bit ADCs," *IEEE Trans. Signal Process.*, vol. 66, no. 5, pp. 1141–1154, March 2018.

[47] C. Wen, C. Wang, S. Jin, K. Wong, and P. Ting, "Bayes-optimal joint channel-and-data estimation for massive MIMO with low-precision ADCs," *IEEE Trans. Signal Process.*, vol. 64, no. 10, pp. 2541–2556, May 2016.

[48] H. Jedda, A. Mezghani, A. L. Swindlehurst, and J. A. Nossek, "Quantized constant envelope precoding with PSK and QAM signaling," *IEEE Trans. Wireless Commun.*, vol. 17, no. 12, pp. 8022–8034, 2018.

[49] E. S. P. Lopes and L. T. N. Landau, "Optimal precoding for multiuser MIMO systems with phase quantization and PSK modulation via branch-and-bound," *IEEE Trans. Wireless Commun. Lett.*, vol. 9, no. 9, pp. 1393–1397, 2020.

[50] I. S. Gradshteyn and I. M. Ryzhik, *Table of integrals, series, and products*, 7th ed. Academic Press, 2007.

[51] W. Rudin, *Real and Complex Analysis*, 3rd ed. New York: McGraw-Hill, 1987.

[52] M. K. Simon, "Single integral representations of certain integer powers of the gaussian Q-function and their application," *IEEE Commun. Lett.*, vol. 6, no. 12, pp. 532–534, 2002.